平成 28 年度学位申請論文

Research on the mechanism that heat preconditioning suppress glucocorticoid-induced muscle atrophy

（温熱刺激によるグルココルチコイド誘導性筋萎縮の進行抑制作用機序の解明に関する実験的研究）

名古屋大学大学院医学系研究科

リハビリテーション療法学専攻

（指導：鈴木　重行　教授）

土田　和可子

Table of contents

Research on the mechanism that heat preconditioning suppress glucocorticoid-induced muscle atrophy

（温熱刺激によるグルココルチコイド誘導性筋萎縮の進行抑制作用機序の解明に関する実験的研究）

Abstract

Synthetic glucocorticoids cause skeletal muscle weakness, and endogenous glucocorticoids levels rise in diseases involving muscle atrophy. Glucocorticoids increase protein degradation and inhibit protein synthesis by catabolic and anabolic pathways, respectively. Heat stress alleviates muscle atrophy and attenuates glucocorticoid-induced muscle effects by unknown mechanisms; therefore, we examined the molecular effects of heat stress against glucocorticoid-induced muscle atrophy. To model skeletal muscle atrophy *in vitro*, we used mouse C2C12 myoblasts differentiated to myotubes and then treated with the synthetic glucocorticoid, dexamethasone. Six hours before dexamethasone treatment, myotubes were exposed to heat stress for 1 hour. In some experiments, myotubes were treated with the PI3K inhibitor, wortmannin 2 hour before heat stress. Myotubes were analyzed morphologically, and mRNA and protein levels of key factors in anabolic and catabolic processes were assessed with real-time RT-PCR and western blotting, respectively.

Dexamethasone decreased myotube diameter and protein content and influenced expression of regulatory factors for both catabolic and anabolic pathways consistent with promoting muscle atrophy. Heat stress prevented morphological and biochemical glucocorticoid effects. For example, heat stress attenuated increases in mRNAs of regulated in development and DNA damage responses 1 (REDD1) and Kruppel-like factor 15 (KLF15), two genes directly targeted by glucocorticoids that decrease protein synthesis by inhibiting mTORC1. In addition, heat stress recovered dexamethasone-induced inhibition of anabolic pathways through PI3K/Akt-dependent mechanisms. Heat stress also normalized dexamethasone-induced increases in key factors promoting protein degradation through the ubiquitin-proteasome system, including FoxO1/FoxO3a and KLF15. Our findings demonstrate the mechanisms by which heat preconditioning may prevent glucocorticoid-induced muscle atrophy, including modulating signaling pathways and expression of several genes targeted by glucocorticoids. This has potentially broad clinical impact because elevated glucocorticoid levels are implicated in a wide range of diseases associated with muscle wasting.

Introduction

Skeletal muscle adapts its mass as a consequence of physical activity, metabolism and hormones. In adulthood, regulation of muscle mass and fiber size essentially reflects protein turnover, namely the dynamic balance between protein synthesis and degradation within the muscle fibers (Sandri, 2008). Muscle hypertrophy occurs when the rate of protein synthesis exceeds the rate of degradation or, conversely, muscle atrophy occurs when the rate of protein synthesis is decreased relative to that of degradation. Thus, muscle atrophy can be caused by either a reduction in the rate of protein synthesis, a rise in the rate of degradation, or a simultaneous decline in synthesis in combination with an increase in degradation. Physical activity, particularly resistance training, induces muscle hypertrophy, characterized by growth of existing myofibers, and often results in health benefits. In contrast, various chronic diseases result in skeletal muscle atrophy, exacerbating the disease and compromising quality of life. Therefore, preventing and attenuating skeletal muscle atrophy is an important clinical goal.

Glucocorticoids (GC) are steroid hormones that respond to a variety of environmental and physiological stimuli. They have wide-ranging regulatory effects on both development and metabolism (Revollo and Cidlowski, 2009). Because of their potent anti-inflammatory and immunosuppressive activities, new GC have been synthesized by the pharmaceutical industry for therapeutic use. Though GC are highly

effective, they have adverse effects including hyperglycemia, weight gain, hypertension, osteoporosis, depression, decreased immunological function and skeletal muscle weakness (Ramamoorthy and Cidlowski, 2013). Many pathological conditions characterized by muscle atrophy, for example sepsis, cachexia, starvation, metabolic acidosis, and severe insulinopenia, are associated with an increase in circulating GC levels (Braun et al., 2013; Braun et al., 2011; Hu et al., 2009; Tiao et al., 1996; Wing and Goldberg, 1993), suggesting that these hormones might have triggered the muscle atrophy observed in these situations.

In skeletal muscle, GC decreased the rate of protein synthesis and increased that of protein breakdown (Goldberg et al., 1980; Lofberg et al., 2002; Tomas et al., 1979), both effects expected to contribute to atrophy. Inhibition of protein synthesis by GC was attributed primarily to inhibition of mammalian target of rapamycin complex 1 (mTORC1), the kinase responsible for the phosphorylation of p70 ribosomal protein S6 kinase 1 (p70S6K1), and eukaryotic translation initiation factor (eIF) 4E binding protein 1 (4E-BP1) (Shah et al., 2000). Repression of mTORC1 signaling has been reported to result in reduction of the initiation phase of mRNA translation with downregulation of protein synthesis (Ma and Blenis, 2009). In recent reports, repression of mTORC1 signaling in response to GC resulted from enhanced transcription of “regulated in development and DNA damage responses 1” (REDD1) and “Kruppel-like factor 15” (KLF15), two repressors of mTORC1 signaling (Shimizu et

al., 2011). These two genes were identified as direct targets of the GC receptor (GR) in skeletal muscle (Shimizu et al., 2011). By inhibiting Akt-mediated inhibitory phosphorylation of proline-rich Akt substrate of 40-kDa (PRAS40), a negative regulator of mTORC1, REDD1 repressed mTORC1 function, leading to decreased phosphorylation of both p70S6K1 and 4E-BP1 (Britto et al., 2014). The action of the transcription factor KLF15 is more complex. By stimulating expression of branched chain amino transferase 2 (BCAT2), an enzyme that degrades branched chain amino acids (BCAA), KLF15 accelerated intracellular catabolism of BCAA, which are believed to activate mTOR and therefore inhibit mTOR activity (Shimizu et al., 2011). In addition, GC mediate anti-anabolic actions by inhibiting phosphatidylinositol 3-kinase (PI3K)/Akt-dependent mTORC1 signaling, which mediates the anabolic actions of insulin-like growth factor 1 (IGF1) (Kuo et al., 2012). Furthermore, glycogen synthase kinase 3β (GSK3β), a downstream target of IGF1/PI3K/Akt signaling that is phosphorylated and inhibited by Akt (Manning and Cantley, 2007), may also be involved in the atrophic effect of GC since it was reported to suppress protein synthesis by inhibiting eIF2B dependent translation (Proud and Denton, 1997).

Besides decreased protein synthesis, GC-induced muscle atrophy involves increased muscle proteolysis signaling. The stimulatory effects of GC on muscle proteolysis have been well studied and two muscle-specific E3 ubiquitin ligases, namely muscle RING finger 1 (MuRF1) and Atrogin-1/muscle atrophy F-box (MAFbx),

were found to play a key role in GC-induced atrophy (Bodine et al., 2001; Sacheck et al., 2004; Wada et al., 2011). Atrogin-1 was shown to function as a ligase for several regulatory proteins such as MyoD and eIF3F (Lagirand-Cantaloube et al., 2008; Tintignac et al., 2005). MuRF1 also functions as a ligase primarily for regulation of several myofibrillar proteins, for example myosin heavy chain (MyHC) (Clarke et al., 2007; Cohen et al., 2009; Polge et al., 2011). Several of these regulatory and myofibrillar proteins are then targeted for degradation through the ubiquitin-proteasome system (UPS). In skeletal muscle, MuRF1 and Atrogin-1 were transcriptionally activated by forkhead box O1 and 3a (FoxO1 and FoxO3a), members of the FoxO family of forkhead transcription factors (Kamei et al., 2004; Sandri et al., 2004; Senf et al., 2008; Waddell et al., 2008). Mechanistically, dephosphorylation, and thus activation, of FoxO1 and FoxO3a would result in their translocation into the nucleus where they can transcriptionally activate MuRF1 and Atrogin-1 to induce atrophy. Activation of IGF1/PI3K/Akt signaling rescued GC-mediated atrophy through phosphorylating and inactivating FoxO1/FoxO3a (Latres et al., 2005; Sandri et al., 2004; Stitt et al., 2004), implicating inhibition of this pathway as a major mechanism behind GC-induced muscle atrophy. In addition to its anti-anabolic functions, KLF15 also has catabolic activity, as indicated by its regulation of expression of MuRF1 and Atrogin-1 (Shimizu et al., 2011). GC-bound GR induced transcription of KLF15, which subsequently interacted with the promoter regions of both MuRF1 and Atrogin-1 to

induce their expression (Shimizu et al., 2011). Furthermore, overexpression of constitutively active forms of both transcription factors additively increased MuRF1 and Atrogin-1 promoter activity and expression (Shimizu et al., 2011). KLF15 overexpression also resulted in increased expression of FoxO1 and FoxO3a, demonstrating further crosstalk among these transcription factors (Shimizu et al., 2011).

Hyperthermia has been widely used as an adjuvant to physical rehabilitation for controlling pain and relieving muscle spasms (Lehmann et al., 1974). Recently, benefits of heat stress for muscle atrophy under various conditions were described (Ichinoseki-Sekine et al., 2014; Luo et al., 2001; Morimoto et al., 2015; Naito et al., 2000; Selsby and Dodd, 2005; Tamura et al., 2015; Yoshihara et al., 2015). Specifically, heat stress attenuated GC-induced muscle atrophy in rats (Morimoto et al., 2015) and prevented GC-induced degradation of proteins in cultured L6 myotubes (Luo et al., 2001). Though the cellular and molecular mechanisms responsible for heat stress-induced suppression of GC-induced muscle atrophy remain unclear, 72-kDa heat shock protein (Hsp72), a heat stress-inducible molecular chaperone, may play a key role in this phenomenon. Interestingly, overexpression of Hsp72 was sufficient to protect against disuse muscle atrophy (Senf et al., 2008). The mechanisms responsible for Hsp72-mediated protection against disuse muscle atrophy appear to be linked to Hsp72-mediated suppression of proteolysis signaling pathways (Senf, 2013). Overall,

available evidence strongly suggest that heat stress can prevent GC-induced proteolysis by inhibiting key atrophy signaling pathways and subsequent muscle atrophy. However, important questions still remain. It is unknown whether heat stress decreases levels of both KLF15 and dephosphorylated FoxO1/FoxO3a, both playing a major role in muscle cell catabolism caused by GC, as well as inducing increases in MuRF1 and Atrogin-1. In addition, the impact of heat stress on GC-mediated inhibition of anabolic pathways during GC-induced muscle atrophy is completely unknown.

In this study, we examined mechanisms underlying the preventive effect of heat stress, applied prior to muscle wasting, against GC-induced muscle atrophy, focusing on anabolic and catabolic signaling pathways. We used cultured C2C12 myotubes, which provide a well-established *in vitro* model system for skeletal muscle atrophy. We found that heat stress could contribute to preventing the deleterious effects of GC by modifying expression of REDD1 and KLF15, two genes directly targeted by GC that can inhibit mTORC1 and subsequently decrease protein synthesis. In addition, the protective effects of heat stress on anti-anabolic actions of GC were partly mediated by the recovered PI3K/Akt signaling. We also found that heat stress normalized GC-affected levels of FoxO1/FoxO3a and MuRF1. Taken together, these results support new mechanisms by which heat preconditioning may prevent GC-induced muscle atrophy.

Materials and Methods

Cell culture

The murine skeletal muscle cell line C2C12 was obtained from the European Collection of Cell Cultures (Salisbury, UK), and maintained as described previously (Iwata et al., 2009). C2C12 myoblasts were cultured at a density of 5×10^3 cells/cm^2 on type I collagen coated 60-mm dishes (Japan BD, Tokyo, Japan). The cells in each dish were grown in 4 ml growth medium consisting of high glucose (4.5 g/l) Dulbecco's Modified Eagle's Medium (DMEM, Sigma-Aldrich, St. Louis, MO, USA) containing 15% (v/v) heat-inactivated fetal bovine serum (Gibco, Carlsbad, CA, USA) and antibiotics (100 U/ml penicillin and 100 μg/ml streptomycin, Gibco) for approximately 48 h, until the myoblasts reached about 90% confluence, in a water-jacketed humidified incubator (MCO-18AIC, Sanyo, Osaka, Japan) equilibrated with 5% CO_2 and 95% air, at 37 °C. To induce spontaneous differentiation by growth factor withdrawal (Yaffe and Saxel, 1977), the growth medium was replaced with differentiation medium consisting of low glucose (1 g/l) DMEM containing 2% (v/v) heat-inactivated horse serum (Gibco). In this medium, the myoblasts fused to form elongated, multi-nucleated myotubes. After 5 days, when approximately 90% of the cells had fused into myotubes, the cultures were treated with 10 μM cytosine ß-D-arabinofuranoside hydrochloride (Ara-C; C6645, Sigma-Aldrich) for 48 h to remove any dividing myoblasts. The myotubes reached a

well-differentiated state showing cross-striation, with a few myotubes displaying spontaneous contractions. The medium was replenished every 48 h during the 5-day differentiation, then once every 24 h after addition of Ara-C and again 2 h before heat treatment. To induce muscle atrophy *in vitro*, cells were treated with the synthetic GC dexamethasone (Dex; D2915, Sigma-Aldrich) in differentiation medium for the indicated times at concentrations indicated in the Results and Figure legends. In some experiments, cells were treated the PI3K inhibitor wortmannin (681675; Merck Millipore, Billerica, MA, USA) 2 h before heat treatment. Wortmannin were maintained during the experiment. Wortmannin was prepared in dimethyl sulfoxide (DMSO) and diluted in differentiation medium to the concentrations indicated in the Results and Figure legends. The final concentration of DMSO never exceeded 0.1% (v/v). When the effect of an inhibitor was being investigated, control cells were treated with DMSO only. After treatments, cells were harvested in appropriate buffers for various analyses or were fixed for morphological analysis, as described further below.

Heat treatment

Heat treatment was performed as modified from a previously described protocol (Welc et al., 2012). C2C12 myotubes were maintained at 37 °C or were treated in a water-jacketed humidified incubator (MCO-18AIC, Sanyo) preset to an elevated temperature (41 °C or, only where indicated, other temperatures) and then, after 60

min exposure to the higher temperature, were returned to the original 37 °C incubator. Once cells were placed in an incubator at 41 °C, it required about 42.5 min for the medium temperature in the dishes to reach the desired experimental temperature (Supplemental Fig. S1A). Control cells were maintained at 37 °C for the entire experiment. After heat treatment, medium in the cells returned to 37 °C after 37.5 min. We previously reported that Hsp72 protein expression in C2C12 myotubes was significantly increased after 4 to 24 h of heat treatment, peaking at 6 h (Tsuchida et al., 2012). Thus, in the current study, a 1-h heat treatment period was used, beginning at 7 h prior to Dex treatment.

Myotube morphological analysis

After treating C2C12 myotubes for 12 or 24 h with Dex, the myotubes were fixed in methanol and stained in Giemsa (109204, Merck Millipore) according to the manufacturer's instructions. Photos were taken at 100 × magnification under a phase contrast microscope (Axio Observer A1, Carl Zeiss, Oberkochen, Germany) with a microscopic camera system (AxioCamHRm, Carl Zeiss). Average diameters of at least 50 myotubes were measured for each condition at three locations 50 μm apart along the length of the myotubes using image editing software (Adobe® Photoshop® CS5, Adobe Systems, CA, USA) as previously described (Stitt et al., 2004). Measurements were conducted in a blinded fashion on coded pictures (control, Dex- or heat stress +

Dex-treated myotubes) of myotubes from each group.

Protein isolation

After indicated treatments, C2C12 myotubes were washed twice with ice-cold phosphate buffered saline (PBS, Sigma-Aldrich) and were harvested with cell scrapers in a whole-cell lysate buffer composed of 200 µl ice-cold RIPA buffer (R0278, Sigma-Aldrich) containing 10% (v/v) protease inhibitor cocktail (P8340, Sigma-Aldrich) and 1% (v/v) phosphatase inhibitor cocktail (524625, Calbiochem, Darmstadt, Germany). Cell lysates were treated with an ultrasonic disintegrator (Bioruptor UCD-200T, Cosmo Bio, Tokyo, Japan) and then centrifuged at 8,000 × g for 10 min at 4 °C. The supernatants were collected and were designated as cell extracts. The total protein content in each cell extract was measured using the BCA protein assay kit (23225, Thermo Fisher Scientific, Waltham, MA, USA) according to the manufacturer's instructions.

Western blot analysis

Each extract was adjusted to a concentration of 2 µg protein per µl with an appropriate volume of RIPA buffer for SDS-PAGE. These samples were each added to an equal volume of EzApply (Atto, Tokyo, Japan) containing 100 mM Tris-HCl buffer (pH 8.8), 2% SDS, 20% sucrose, 0.06% bromophenol blue and 100 mM DTT and heated

at 95 °C for 5 min. For SDS-PAGE, samples containing 10-30 µl protein were loaded per lane and separated on precast polyacrylamide gradient (7.5-12%, Bio-Rad, Hercules, CA, USA) gels at 200 V for 30 min. Proteins were then transferred from the gel to 0.2-µm polyvinylidene difluoride membranes (Bio-Rad) by electro-blotting at a constant current of 1.3 A for 7 min using a rapid transfer system (Trans-Blot Turbo, Bio-Rad). After transfer, western blot analysis was performed with a protein detection system (SNAP i.d. 2.0, Merck Millipore). The blots were blocked with 0.5% (w/v) nonfat dried milk or 1% (w/v) bovine serum albumin diluted in Tris-buffered saline containing 0.1% (v/v) Tween 20 (TBS-T), to block nonspecific reactions, and then incubated overnight at 4 °C with the indicated primary antibodies. These antibodies were directed against Hsp72 (ADI-SPA-812, Enzo Life Sciences, Farmingdale, NY, USA), phosphorylated Akt (Thr308; #2965, Cell Signaling Technology, Danvers, MA, USA), Akt (#4691, Cell Signaling Technology), phosphorylated p70S6K1 (Thr389; #9206, Cell Signaling Technology), p70S6K1 (#2708, Cell Signaling Technology), phosphorylated GSK3β (Ser9; #5558, Cell Signaling Technology), GSK3β (#9832, Cell Signaling Technology), phosphorylated mitogen-activated protein kinase kinase 1/2 (MEK1/2) (Ser217/221; #9154, Cell Signaling Technology), MEK1/2 (#9122, Cell Signaling Technology), phosphorylated extracellular signal-regulated kinase 1/2 (ERK1/2) (Thr202/Tyr204; #4370, Cell Signaling Technology), ERK1/2 (#4696, Cell Signaling Technology), phosphorylated FoxO1 (Thr256; #9461, Cell Signaling Technology),

FoxO1 (#2880, Cell Signaling Technology), phosphorylated FoxO3a (Ser253; ab47285, Abcam, Cambridge, MA, USA), FoxO3a (#2497, Cell Signaling Technology), MyHC fast (MyHC-f) (M4276, Sigma-Aldrich), total MyHC (MF20, Developmental Studies Hybridoma Bank, Iowa, IA, USA), and ß-actin (#5125, Cell Signaling Technology). The blots were washed, incubated with the respective secondary antibodies and washed again. The immunostained bands were visualized using the ECL Prime Western Blotting Detection System (RPN2232, GE Healthcare Japan, Tokyo, Japan) according to the manufacturer's instructions. Illumination patterns were measured using a high sensitivity cooled CCD camera (Light Capture II, Atto) to obtain an image of the target protein bands. Subsequent quantification of band images was achieved using image analysis software (CS analyzer 3.0, Atto).

RNA isolation and assessment of mRNA expression by real-time quantitative RT-PCR

C2C12 myotubes were washed twice with PBS and total RNA was isolated using the PureLink® RNA Mini Kit (Life Technologies, Grand Island, N.Y, USA) according to the manufacturer's instructions. RNA concentrations were measured using a Nanodrop ND-1000 UV-Vis spectrophotometer (Thermo Scientific, Wilmington, DE, USA). Next, total RNA was reverse transcribed into cDNA using the High-Capacity RNA-to-cDNA™ Kit (Life Technologies) and a 2720 thermocycler (Life Technologies), according to the manufacturer's instructions. Quantitation of gene

expression was determined by real-time quantitative reverse transcription PCR (qRT-PCR). qRT-PCR reactions contained 2 µl cDNA (50 µg/µl), 10 µl TaqMan® Fast Advanced Master Mix (Life Technologies) and 1 µl primers. PCR reaction analysis was performed by a StepOnePlus Real-Time PCR system (Life Technologies) using the ΔΔCt method. The primers were as follows: Hsp72 (Mm01159846_s1), REDD1 (Mm00512504_g1), REDD2 (Mm00513313_m1), KLF15 (Mm00517792_m1), FoxO1 (Mm00490672_m1), FoxO3a (Mm01185722_m1), Atrogin-1 (Mm00499523_m1), MuRF1 (Mm01185221_m1), and glyceraldehyde-3-phosphate dehydrogenase (GAPDH; Mm99999915_g1) by TaqMan Gene Expression Assays (Life Technologies). GAPDH was used as endogenous control to normalize the samples.

Statistical analysis

Statistical analyses were performed using SPSS version 15.0 (SPSS Inc., Chicago, IL, USA). All values are presented as means ± standard deviation (SD). The data were analyzed using the Mann-Whitney U-test for comparisons between two conditions and Kruskal-Wallis test followed by Steel's test for comparisons with controls, and Steel-Dwass test for multiple comparisons. Differences between conditions were considered statistically significant at $P < 0.05$.

Results

Dex treatment caused atrophy of C2C12 myotubes

We first examined the dose-dependent effects of the synthetic GC Dex by assessing myotube diameter. Compared with untreated controls (n = 55, myotube diameter 18.7 ± 4.5 μm), fully differentiated C2C12 myotubes treated with Dex for 24 h showed a distinct atrophic phenotype (Fig. 1A), with a dose-dependent decrease in myotube diameter (Fig. 1B). In myotubes treated with Dex at 0.01 μM, there was no significant effect but a trend toward a 2% decrease in diameter (n = 54, 18.3 ± 4.9 μm), with a similar trend of a 10% decrease with 0.1 μM Dex (n = 53, 16.8 ± 4.2 μm). Myotube diameters were decreased significantly, however, by 18% with 1 μM (n = 51, 15.4 ± 3.1 μm) and by 23% with 10 μM (n = 54, 14.4 ± 3.5 μm) or 100 μM (n = 54, 14.5 ± 3.5 μm) Dex ($P < 0.05$) (Fig. 1B). Based on this, 10 μM Dex was used in subsequent experiments to induce atrophy in C2C12 myotubes.

Next, we examined the time dependence of the effect of Dex (10 μM) treatment on C2C12 myotube diameter. Compared with controls, the diameters of myotubes treated with Dex were not changed at 12 h but showed a significant decrease, 24%, at 24 h (Fig. 1C). We also measured contents of total protein, MyHC-f and total MyHC in C2C12 myotubes treated with Dex for 12 and 24 h. Similar to its effect on diameter, Dex treatment significantly decreased the total protein content by 16% (Fig. 1D), MyHC-f content by 21% (Figs. 1E and F), and total MyHC content by 24% at 24 h, compared with levels in controls (Figs. 1E and G), but showed no changes at 12 h.

These results indicated that the *in vitro* response of C2C12 myotubes to Dex treatment recapitulated the *in vivo* response of skeletal muscle (Clarke et al., 2007; Hickson and Davis, 1981; Ma et al., 2003; Yamamoto et al., 2010). In addition, the data for C2C12 myotubes were consistent with previous reports that Dex decreased myotube diameter (Chromiak and Vandenburgh, 1992; Kukreti et al., 2013; Latres et al., 2005; Menconi et al., 2008; Sandri et al., 2004; Stitt et al., 2004) total protein (Chromiak and Vandenburgh, 1992; Polge et al., 2011; Sacheck et al., 2004; Stitt et al., 2004; Wada et al., 2011), and/or myofibrillar protein content (Chromiak and Vandenburgh, 1992; Clarke et al., 2007; Verhees et al., 2011) *in vitro*.

Dex treatment induced increases in REDD1, KLF15, FoxO1, FoxO3a, MuRF1, and Atrogin-1 mRNA expression in C2C12 myotubes

It was previously shown that REDD1, REDD2, and KLF15, upstream negative effectors of mTORC1 signaling, induced muscle atrophy via inhibition of protein synthesis (Britto et al., 2014; Kelleher et al., 2013; Shimizu et al., 2011; Wang et al., 2006). It was also reported that MuRF1 and Atrogin-1, which play key roles in muscle proteolysis, were transcriptionally activated by KLF15, FoxO1, and FoxO3a in response to Dex treatment (Kamei et al., 2004; Sandri et al., 2004; Shimizu et al., 2011; Waddell et al., 2008). Therefore, we assessed the mRNA expression of these regulatory factors in fully differentiated C2C12 myotubes undergoing Dex-induced skeletal

muscle atrophy. REDD1 mRNA expression rapidly increased by 3.1-fold at 1 h, reached a peak of 3.6-fold increase at 3 h and gradually decreased at 6-24 h of Dex (10 μM) treatment (Fig. 2A). In contrast, REDD2 mRNA expression was unchanged throughout the entire Dex treatment period (Fig. 2B). KLF15 mRNA expression increased by 3.2- and 5.2-fold at 1 and 3 h, respectively, and reached a 6.3-fold peak at 6 h of Dex treatment (Fig. 2C). FoxO1 mRNA expression was increased by 1.2-fold, though this increase was observed at only 1 h of Dex treatment (Fig. 2D). FoxO3a mRNA expression increased by 1.3-fold at 1 h and reached a 2.0-fold peak at 3 h of Dex treatment (Fig. 2E). MuRF1 mRNA expression gradually increased by 1.2- and 1.6-fold at 1 and 3 h, respectively and reached a 2.0-fold peak at 6 h of Dex treatment (Fig. 2F). Atrogin-1 mRNA expression did not increase at 1 h, but rapidly increased to 1.7-fold at 3 h of Dex treatment, remaining stable at 1.7- to 1.8-fold at later times (Fig. 2G). These results show that peak increases in expression of REDD1, a key regulator of protein synthesis, were observed at 3 h of Dex treatment. Hence, for subsequent experiments, we analyzed C2C12 myotubes at 3 h of Dex treatment to investigate changes in the anabolic markers, REDD1, KLF15, Akt, p70S6K1, and GSK3β, during Dex-induced atrophy. The time point showing peak changes in MuRF1 and Atrogin-1, both considered as rate-limiting enzymes of UPS-mediated muscle protein breakdown, was observed at 6 h of Dex treatment. Therefore, we analyzed C2C12 myotubes at 6 h of Dex treatment to investigate changes in the catabolic markers, KLF15, Akt, FoxO,

MuRF1, and Atrogin-1, during Dex-induced atrophy.

Having observed increases in REDD1 and KLF15 expression during Dex-induced atrophy, we next investigated how REDD1 and KLF15 expression could be further regulated during this process. Because Dex is a synthetic GC, it signals by binding to the GR, which then translocates into the nucleus to regulate expression of target genes (Kadmiel and Cidlowski, 2013). To confirm that GR was involved in the Dex-mediated upregulation of REDD1 and KLF15 mRNA expression, we treated fully differentiated C2C12 myotubes with the GR-specific antagonist RU486 and assessed REDD1 and KLF15 mRNA expression in response to Dex treatment. Treatment of myotubes with RU486 prevented Dex-induced increases in REDD1 and KLF15 mRNA expression (Supplemental Figs. S2A and B). These results indicated that REDD1 and KLF15 expression was mediated by the GR in Dex-induced atrophy.

Heat stress suppressed Dex-induced muscle atrophy

In previous studies, heat stress attenuated the Dex-induced decrease in muscle fiber diameter of extensor digitorum longus muscle *in vivo* in rats (Morimoto et al., 2015) and suppressed Dex-induced muscle proteolysis in L6 myotubes *in vitro* (Luo et al., 2001). These effects were attributed to Hsp72 induced by heat stress. Therefore, to investigate whether heat stress induced Hsp72 mRNA and protein expression under our experimental conditions, we exposed fully differentiated C2C12 myotubes to heat

stress. Treating C2C12 myotubes at 39, 40, or 41 °C increased Hsp72 mRNA expression by 1.5-, 3.5-, and 6.0-fold, respectively, when measured immediately after heat treatment (Supplemental Fig. S1B). Afterwards, Hsp72 mRNA expression gradually decreased over time reaching control levels at 5 h after heat treatment. In addition, Hsp72 protein expression was significantly increased, 2.2- and 4.7-fold at 39 and 41 °C, respectively, at 6 h of heat treatment, as compared with control myotubes maintained at 37 °C (Supplemental Figs. S1C and D). These results indicated that heat stress-induced increases in Hsp72 mRNA and protein expression were temperature-dependent. Accordingly, heat treatment at 41 °C, which induced sufficient levels of Hsp72 expression, was used for subsequent experiments to investigate how heat stress can influence Dex-induced effects.

We next investigated whether heat stress was sufficient to overcome Dex-induced atrophy in C2C12 myotubes. Fully differentiated C2C12 myotubes were exposed to heat stress (at 41 °C for 60 min) ending 6 h prior to treatment with Dex (10 μM) for 24 h. The Dex treatment caused a 25% decrease in diameter in C2C12 myotubes maintained at normal temperature, but this effect was abolished in myotubes that had undergone heat stress (Fig. 3A). As shown in Fig. 3B, compared with untreated controls, C2C12 myotubes treated with Dex had a lower percentage of large muscle fibers (> 20 μm) and a higher percentage of small fibers (> 10 μm). Both Dex-induced effects were suppressed in myotubes that had been subjected to heat

stress. We investigated whether heat stress blocked Dex-induced MyHC-f loss in C2C12 myotubes. Dex treatment resulted in a loss of 28% of MyHC-f content, an effect also abolished by heat stress (Figs. 3C and D). Overall, these results suggested that heat stress suppressed Dex-induced decreases in both myotube diameter and myofibrillar protein content. We further investigated whether Hsp72 protein expression was increased by heat stress in Dex-treated C2C12 myotubes. In C2C12 myotubes that had been exposed to heat stress (at 41 °C for 60 min) 6 h prior to Dex treatment, Hsp72 protein expression was increased 3.0-, 2.9-, 3.4-, and 2.1-fold at 3, 6, 12, and 24 h, respectively, of Dex treatment (Figs. 4A and B). These observations indicate that heating at 41 °C for 60 min induced a sustained increase in Hsp72 protein expression throughout the period of Dex treatment in C2C12 myotubes.

Heat stress suppressed Dex-induced increases in REDD1 and KLF15 mRNA expression and decreases in phosphorylated Akt, p70S6K1, and GSK3β protein levels in C2C12 myotubes

To elucidate effects of heat stress on Dex-mediated inhibition of anabolic pathways, we measured mRNA expression of REDD1 and KLF15, both factors that inhibit mTORC1 signaling (Britto et al., 2014; Shimizu et al., 2011), in C2C12 myotubes treated with Dex (10 μM) for 3 h. REDD1 mRNA expression increased by 3.6-fold in Dex-treated C2C12 myotubes, an effect blunted by heat stress (Fig. 5A).

Similarly, Dex-induced a 4.8-fold increase in KLF15 mRNA expression, also attenuated by heat stress (Fig. 5B). We next examined Akt phosphorylated on Thr308, because REDD1-mediated inhibition of mTORC1 was found to involve Akt dephosphorylation at this site (Britto et al., 2014). Dex treatment resulted in a 30% decrease in phosphorylated Akt on Thr308 in myotubes with no change in total Akt protein (Figs. 5C-E). This effect was inhibited by heat stress (Figs. 5C-E). We also examined mTORC1 activity by evaluating phosphorylation of p70S6K1 at the mTOR-specific site Thr389 (Brown et al., 1995; Brunn et al., 1997). Similar to the observations with Akt, Dex treatment resulted in a 29% decrease in phosphorylated p70S6K1 at Thr389, with no change in total p70S6K1 protein, and heat stress prevented this effect (Figs. 5C, F, and G). Because Akt is known to reduce GSK3β kinase activity through phosphorylation of Ser9 (Manning and Cantley, 2007), resulting in increased initiation of mRNA translation and capacity to promote protein synthesis (Proud and Denton, 1997), we further analyzed levels of phosphorylated GSK3β in Dex-treated C2C12 myotubes, with/without heat stress. As expected, we observed a 34% decrease in phosphorylated GSK3β on Ser9 after Dex treatment, with no change in total GSK3β protein (Figs. 5C, H, and I). This effect, too, was inhibited by heat stress (Figs. 5C, H, and I).

Dex treatment and heat stress did not alter the levels of phosphorylated and total

MEK1/2 and ERK1/2 in C2C12 myotubes

The MEK/ERK signaling pathway has been proposed to enhance protein synthesis by regulating ribosomal RNA gene expression (Stefanovsky et al., 2006). Recent studies have also reported that the MEK/ERK-dependent pathway may contribute to the maintenance of skeletal muscle mass by modulating Akt signaling (Shi et al., 2009). Based on these findings, we examined the phosphorylation states of MEK1/2 at Ser217/221 sites and the downstream effector ERK1/2 at Thr202/Tyr204 sites in our atrophy model. Treatment of C2C12 myotubes with Dex for 3 h did not affect the levels of phosphorylated and total MEK1/2 and ERK1/2 (Figs. 6A-E). This is consistent with a previous study showing that Dex had no effect on the signaling pathway (Gwag et al., 2013). Similarly, heat stress did not alter the levels of phosphorylated and total MEK1/2 and ERK1/2 in Dex-treated C2C12 myotubes (Figs. 6A-E). These results support the hypothesis that the MEK/ERK signaling pathway is not involved in the Dex-induced inhibition of protein synthesis and heat stress-induced anti-atrophic effects under the present experimental conditions.

Heat stress normalized Dex-induced decreases in phosphorylated Akt, p70S6K1, and GSK3β through PI3K-dependent mechanisms

Recent studies have shown that Dex can exert their anti-anabolic actions by inhibiting PI3K/Akt-dependent mTORC1 signaling (Kuo et al., 2012). To determine

whether heat stress suppressed the Dex-induced inhibition of anabolic pathways through the PI3K/Akt signaling pathway, we determined how wortmannin, a PI3K inhibitor, affected the basal phosphorylation status of direct downstream targets of PI3K, including Akt (Thr308), p70S6K1 (Thr389), and GSK3β (Ser9) in non-Dex treated myotubes. Relatively low concentrations of wortmannin (10-100 nM) had no effect, whereas relatively high concentrations (0.5-10 μM) decreased phosphorylated Akt, p70S6K1, and GSK3β (Supplemental Figs. S3A-G). Based on the initial dose-ranging experiment, 100 nM wortmannin was chosen for all further experiments to investigate whether PI3K is required for the heat stress suppression of Dex-induced decreases in phosphorylated Akt, p70S6K1, and GSK3β. Fully differentiated C2C12 myotubes were treated with 100 nM wortmannin 2 h before heat treatment, and were exposed to heat stress (at 41 °C for 60 min) ending 6 h prior to treatment with Dex for 3 h. Wortmannin were required to completely abolish the inhibitory effect of heat stress on Dex-induced decreases in phosphorylated Akt, p70S6K1, and GSK3β with no change in each total protein levels (Figs. 7A and C-H). These observations indicated that heat stress may normalize the Dex-induced inhibition of anabolic pathways through PI3K-dependent mechanisms. We confirmed that wortmannin did not inhibit the heat stress-induced increase in Hsp72 protein expression in Dex-treated C2C12 myotubes (Figs. 7A and B). We also confirmed that wortmannin did not alter the levels of phosphorylated and total MEK1/2 and ERK1/2 in Dex-treated C2C12 myotubes

with/without heat stress (Supplemental Fig. S4A-E).

Heat stress partially attenuated Dex-induced decreases in myotube diameter through PI3K-dependent mechanisms

Because wortmannin blocked the inhibitory effect of heat stress on Dex-induced decreases in phosphorylated Akt, p70S6K1, and GSK3β, we next examined whether PI3K is required for the anti-atrophic effects of heat stress by evaluating myotube diameter. Fully differentiated C2C12 myotubes were treated with 100 nM wortmannin 2 h before heat treatment, and were exposed to heat stress (at 41 °C for 60 min) ending 6 h prior to treatment with Dex for 24 h. Wortmannin did not affect diameter of C2C12 myotubes with/without Dex treatment (Figs. 8A-B). However, wortmannin attenuated, but did not abolish, the inhibitory effect of heat stress on Dex-induced decreases in myotube diameter (Figs. 8A-B). These results indicated that heat stress may at least partially attenuated Dex-induced decreases in myotube diameter through PI3K-dependent mechanisms.

Heat stress suppressed Dex-induced increases in KLF15 and MuRF1 mRNA expression, decreases in phosphorylated Akt, FoxO1, and FoxO3a protein levels, and increase in total FoxO1 and FoxO3a in C2C12 myotubes

In addition to its anti-anabolic function, KLF15, whose expression is induced

by Dex treatment, interacts with the promoter regions of both MuRF1 and Atrogin-1 to induce their expression (Shimizu et al., 2011). Moreover, overexpression of constitutively active forms of KLF15 resulted in increased expression of FoxO1 and FoxO3a (Shimizu et al., 2011). Our results show that KLF15 increased by 6.2-fold in C2C12 myotubes at 6 h Dex treatment (Fig. 9A), corresponding with an increased total FoxO1 (1.2-fold, $P = 0.0644$) and FoxO3a (1.5-fold, $P < 0.05$) protein levels observed at this time point (Figs. 9B, F, and H). These increases were prevented by heat stress.

Dephosphorylation and, thus, activation of FoxO1 and FoxO3a, by dephosphorylating and inactivating Akt, resulted in MuRF1 and Atrogin-1 mRNA expression, inducing atrophy (Sandri et al., 2004; Stitt et al., 2004). We therefore further confirmed levels of phosphorylated Akt, FoxO1 and FoxO3a in C2C12 myotubes treated with Dex for 6 h. Dex treatment resulted in a significant decrease, 32%, in levels of Akt phosphorylated on Thr308. This was inhibited by heat stress (Figs. 9B-D). Dex treatment also resulted in a significant decrease in the phosphorylation levels of both FoxO1 on Ser256 (48%) and FoxO3a on Ser253 (49%) both effects also reduced by heat stress (Figs. 9B, E, and G). Because FoxO1/FoxO3a can induce expression of MuRF1 and Atrogin-1, we performed qRT-PCR and found increased abundance of mRNA for MuRF1 (1.9-fold) and Atrogin-1 (1.6-fold) after Dex treatment. Consistent with the above results, the increase in MuRF1 observed in response to Dex treatment was attenuated by heat stress (Fig. 9I). However, heat stress did not block the

Dex-induced increase in Atrogin-1 mRNA expression (Fig. 9J).

Discussion

Our study provided evidence that heat stress can prevent GC-mediated muscle atrophy and upregulation of direct target genes of GC and that these heat stress effects may be, at least in part, regulated by Hsp72. These observations are important from a clinical standpoint because high GC levels, as seen in patients with Cushing's syndrome and in patients treated with corticosteroids for asthma and rheumatoid arthritis, have been associated with muscle wasting and weakness (Bowyer et al., 1985; Carroll and Findling, 2010; Minetto et al., 2011; Seale and Compton, 1986). In addition, loss of muscle mass under various catabolic conditions, including sepsis and cachexia, was in part mediated by GC (Braun et al., 2013; Braun et al., 2011; Hu et al., 2009; Tiao et al., 1996; Wing and Goldberg, 1993). Thus, our results suggest that multiple patient groups suffering from GC-dependent muscle wasting may benefit from heat stress.

In several previous reports, cultured myotubes treated with the synthetic GC Dex served as an *in vitro* model of GC-induced muscle atrophy. The concentration of Dex used in those studies varied substantially, with effective concentrations ranging from 10-50 nM (Du et al., 2000; Thompson et al., 1999) to 10-100 μM (Clarke et al., 2007; Kukreti et al., 2013; Latres et al., 2005; Stitt et al., 2004; Verhees et al., 2011;

Wada et al., 2011; Wright et al., 2015). In our study, we found that C2C12 myotubes treated with Dex for 24 h exhibited a dose-dependent reduction of diameter at 0.1-100 μM Dex. Our results also showed that treating myotubes with 10 μM Dex for 24 h was sufficient to significantly decrease myotube diameter and myofibrillar proteins (total protein, MyHC-f, and total MyHC protein levels). These results are consistent with previous reports in which Dex impaired myotube formation, muscle-specific protein expression and protein turnover in C2C12 myotubes (Polge et al., 2011; Sacheck et al., 2004; Verhees et al., 2011; Wright et al., 2015). In an *in vivo* rat study, heat stress attenuated atrophy of the extensor digitorum longus muscle caused by Dex (Morimoto et al., 2015). In agreement with this, heat stress almost completely prevented Dex-induced effects on myotube diameters and myofibrillar protein abundance in our experiments. This led us to examine mechanisms underlying the effects of heat stress, focusing on phosphorylation and expression of key molecules involved in regulating protein synthesis and degradation in response to GC.

Biochemically, GC was found to increase the rate of protein breakdown and decrease the rate of protein synthesis, thus contributing to a loss of muscle mass (Goldberg et al., 1980; Lofberg et al., 2002; Tomas et al., 1979). GC elicited atrophy of muscle by increasing the rate of protein degradation, primarily by the UPS. Protein synthesis was also suppressed at the level of translational initiation, preventing production of new myofibrillar proteins (Braun and Marks, 2015).

GC reduced initiation of translation and protein synthesis in skeletal muscle within hours of administration (Ma and Blenis, 2009). The inhibition of protein synthesis by GC primarily resulted from inhibition of mTORC1, the kinase responsible for phosphorylation of p70S6K1 and 4E-BP1 (Shah et al., 2000). Several studies showed that REDD1 acted as an upstream suppressor of mTORC1 signaling (Brugarolas et al., 2004; DeYoung et al., 2008; Favier et al., 2010; Lin et al., 2005; McGhee et al., 2009; Protiva et al., 2008; Shoshani et al., 2002; Sofer et al., 2005; Wang et al., 2006). Though its mechanism of action has not been well characterized, adverse conditions such as ATP depletion (Sofer et al., 2005), DNA damage (Lin et al., 2005) endoplasmic reticulum stress (Protiva et al., 2008), hypoxia (Brugarolas et al., 2004; DeYoung et al., 2008; Favier et al., 2010; Shoshani et al., 2002), starvation (McGhee et al., 2009), and GC treatment (Wang et al., 2006) transcriptionally induced REDD1 expression and inhibited mTORC1 signaling by promoting dephosphorylation of Akt on Thr308 (Britto et al., 2014; Dennis et al., 2014). In our study, we observed upregulation of REDD1 in Dex-treated myotubes, concomitant with a decrease in phosphorylation of Akt on Thr308 and p70S6K1 at the mTORC1-dependent site Thr389. This indicated that the increased levels of REDD1 detected following Dex treatment may have caused the hypophosphorylation of both Akt and p70S6K1. Importantly, heat stress blocked Dex-induced induction of REDD1 expression and reduction in phosphorylated Akt and p70S6K1. These data are in agreement with previously published results from Britto

et al. (2014), who demonstrated that deletion of the REDD1 gene prevented Dex-induced muscle atrophy by suppressing mTORC1 and inhibition of protein synthesis through a mechanism involving Akt. Therefore, we propose that one of the mechanisms by which heat stress can exert protective effects against Dex-induced muscle atrophy is through inhibiting the increase in REDD1 caused by Dex.

Phosphorylated Akt activated mTORC1 (Sandri, 2008) and, in parallel, inactivated GSK3β (Manning and Cantley, 2007), resulting in increased mRNA translation initiation and, thereby, capacity to promote protein synthesis (Ma and Blenis, 2009; Proud and Denton, 1997). GSK3β is a signaling protein directly downstream of Akt. Akt was shown to reduce GSK3β kinase activity through phosphorylation of Ser9, resulting in enhanced mRNA translation due to increased eIF2B activity (Manning and Cantley, 2007). Interestingly, inhibition of GSK3β by overexpression of a dominant negative GSK3β, small interfering RNA, or pharmacologic inhibitors prevented muscle protein loss and atrophy caused by GC *in vitro* (Evenson et al., 2005; Fang et al., 2005; Verhees et al., 2011) and *in vivo* (Schakman et al., 2008), indicating that muscle atrophy caused by GC was dependent on GSK3β. Consistent with this, heat stress prevented the reduced phosphorylation of Akt and GSK3β and myotubular atrophy in Dex-treated C2C12 myotubes in our experiments. Thus, it is possible that prevention by heat stress of Dex-mediated inhibition of GSK3β phosphorylation that we observed reflected, at least in part,

normalization of levels of phosphorylated Akt. Such alterations would be expected to explain how heat stress can override the anti-anabolic action of Dex in skeletal muscle.

Dex reduces PI3K/Akt-dependent mTORC1 signaling by increasing the p85α regulatory subunit for PI3K, leading to protein synthesis inhibition (Kuo et al., 2012). We demonstrated the role of PI3K in the protective effect of heat stress using the PI3K inhibitor, wortmannin. PI3K was critical for the protective effects of heat stress on anabolic signaling pathways, which included Akt, p70S6K1, and GSK3β, in our atrophy model. Although heat stress increased the phosphorylation of anabolic signaling molecules in the Dex-induced model of C2C12 myotube atrophy, heat stress-induced Akt phosphorylation at Ser308 was rapid (10 min) and transient (returned to basal levels by 60 min after heat stress in non-Dex treated myotubes, data not shown). These data are in agreement with recently published results from Yoshihara *et al.* (2016), which reported a significant increase in Akt phosphorylation at Thr308 immediately after heat stress treatment in rat skeletal muscle. Thus, when investigating the protective effects of heat stress on anabolic signaling pathways, the increased effect on phosphorylated Akt may be lost in myotubes. These suggest the possibility that heat stress is restores rather than stimulates PI3K/Akt signaling pathways inhibited by Dex. We evaluated myotube diameter to determine whether heat stress suppressed Dex-induced C2C12 myotubes atrophy through PI3K-dependent mechanisms. Wortmannin attenuated the protective effect of heat

stress on Dex-induced decreases in myotube diameter; however, it did not completely abolish these effects of heat stress. Thus, the anti-atrophic effects of heat stress on Dex-treated myotubes were, at least in part, mediated by normalizing PI3K/Akt signaling. Taken together, heat stress may prevent Dex-induced muscle atrophy via regulating PI3K/Akt signaling pathways and modulating catabolic signaling pathways and the expression of REDD1 and KLF15 targeted by Dex.

Regarding the mechanistic basis of the catabolic regulation, the FoxO family of transcription factors is known to play a pivotal role in muscle cells (Milan et al., 2015). The phosphorylation of FoxO by Akt led to its inactivation in the cytosol. However, the inhibition of the IGF1/PI3K/Akt signaling pathway by GC triggered dephosphorylation of FoxO and its import to the nucleus (Sandri et al., 2004; Stitt et al., 2004). The activation of Akt and inactivation of FoxO would reduce activity of the UPS and, consequently, decrease protein degradation. Therefore, in catabolic states, where IGF1/PI3K/Akt signaling is impaired, muscle atrophy may arise through increased activity of FoxO and activation of MuRF1 and Atrogin-1 transcription (Bonaldo and Sandri, 2013). In agreement with this idea, in our study, we observed a decrease in levels of phosphorylated Akt, FoxO1, and FoxO3a in C2C12 myotubes treated with Dex, concomitant with upregulation of MuRF1 and Atrogin-1. Importantly, however, heat stress restored control levels of phosphorylated Akt, FoxO1, and FoxO3a and also reduced MuRF1 levels during Dex-induced muscle atrophy. Thus, these data suggest

that the anti-atrophic effects of heat stress on Dex-treated myotubes were likely mediated by negative regulation of FoxO1/FoxO3a through protected phosphorylation of Akt.

A surprising finding of our study was that heat stress did not suppress Dex-induced Atrogin-1 expression, despite strongly attenuating MuRF1 mRNA levels. The reason for this is unclear but one possible explanation is that MuRF1 and Atrogin-1 mediated ubiquitination of distinct protein substrates. MuRF1 is known to ubiquitinate several muscle structural proteins, including MyHC (Clarke et al., 2007), myosin binding protein C, myosin light chains 1 and 2 (Cohen et al., 2009), and actin (Polge et al., 2011). In contrast, the identified substrates of Atrogin-1 appear to be involved in growth-related processes or survival pathways. Atrogin-1 promotes ubiquitination and degradation of MyoD (Tintignac et al., 2005), a key muscle transcription factor, and of eIF3F (Lagirand-Cantaloube et al., 2008), an important protein synthesis activator. Moreover, valuable information on the role of specific components of the UPS in muscle has been obtained using genetically modified animals. Mice lacking Atrogin-1 and MuRF1 were resistant to muscle atrophy induced by denervation (Bodine et al., 2001). In contrast, Atrogin-1 knockdown prevented muscle loss during fasting (Cong et al., 2011), whereas MuRF1 knockout, but not Atrogin-1 knockout, mice were resistant to GC-induced muscle atrophy (Baehr et al., 2011). These observations demonstrated that MuRF1 and Atrogin-1 would not function

similarly in all atrophy models and that the inhibition of MuRF1 expression by heat stress may be sufficient to attenuate muscle proteolysis during Dex-induced muscle atrophy, without inhibiting Atrogin-1 expression.

Interestingly, we report here that KLF15 was increased by Dex treatment, but was remarkably decreased by heat stress. Research over the past 10 years has uncovered the importance of KLF15 in skeletal muscle metabolism for both amino acid catabolism and lipid utilization (Manring et al., 2014). Its role in metabolism may contribute to its association with GC-induced muscle atrophy. The mechanism by which KLF15 contributes to protein catabolism is not completely understood but KLF15 was found to activate BCAT2, which is responsible for degradation of BCAA (Shimizu et al., 2011). Accelerated BCAA degradation led to a decrease in mTORC1 activity (Lang et al., 2010). Further analysis indicated that KLF15 can participate in muscle catabolism via transcriptional upregulation of FoxO1/FoxO3a, MuRF1, and Atrogin-1 (Shimizu et al., 2011). These studies also demonstrated that KLF15 and FoxO1 cooperated to upregulate MuRF1 and Atrogin-1 expression. Taken together, KLF15 can apparently contribute to GC-induced muscle atrophy by altering the ratio of protein degradation and synthesis. Thus, though the precise mechanism underlying heat stress-induced suppression of KLF15 expression in myotubes remains unclear, it is conceivable that the beneficial effects of heat stress on muscle protein degradation and synthesis are closely associated with inhibition of KLF15 expression.

Heat stress attenuated reductions in soleus muscle mass and fiber size in various animal models (Naito et al., 2000; Selsby and Dodd, 2005), and it appears likely that Hsp72 would play a protective role in heat stress-induced suppression of muscle atrophy. It is possible that the molecular chaperone and protein repair functions of Hsp72 can protect against muscle atrophy, though several other mechanisms might also account for this protection. Another mechanism responsible for Hsp72-mediated protection against muscle atrophy has been linked to the Hsp72-mediated suppression of the proteolytic signaling pathway, including FoxO. Specifically, a study in C2C12 myotubes showed that Hsp72 bound to phosphorylated Akt, protecting it from dephosphorylation, thus maintaining FoxO3a in its phosphorylated, inactive state (Kukreti et al., 2013). Furthermore, a recent *in vivo* study demonstrated that atrophy of the soleus muscle was remarkably attenuated when plasmid-mediated overexpression of Hsp72 abolished the transcriptional activity of FoxO3a (Senf et al., 2008). Another mechanism by which Hsp72 can offer resistance to atrophy is through associating directly with GR in the cytoplasm, thereby preventing nuclear translocation of GR (Dittmar and Pratt, 1997; Kukreti et al., 2013). Our results demonstrated that heat stress increased Hsp72 expression during Dex treatment of C2C12 myotubes and prevented Dex-induced myotube atrophy. Hence, such heat stress-induced increases in Hsp72 could contribute to the observed protection against Dex-induced myotube atrophy. However, future studies employing

in vitro and *in vivo* modification of the Hsp72 gene, for example, by gene knockout or knockdown, will be required to build solid understanding of the mechanism of the beneficial effects of heat stress against GC-induced muscle atrophy.

In conclusion, our study is important because it clarifies some of the mechanisms underlying the ability of heat stress, applied prior to muscle wasting, to prevent GC-induced muscle atrophy. Our data provide the first evidence that, during Dex treatment of myotubes, heat stress can normalize expression of REDD1 and KLF15, direct GC target genes that inhibit mTORC1 and subsequently decrease protein synthesis, and FoxO1/FoxO3a and KLF15, key factors orchestrating UPS and increasing proteolysis. Heat stress can also recover, at least in part, the negative effects of Dex on anabolic pathways and myotube atrophy through PI3K-dependent mechanisms. Understanding the cellular basis of GC-induced skeletal muscle atrophy will enable the rational development of therapeutic interventions to minimize the debilitating effects of the muscle atrophic response to GC.

Literature Cited

Baehr LM, Furlow JD, Bodine SC. 2011. Muscle sparing in muscle RING finger 1 null mice: response to synthetic glucocorticoids. The Journal of physiology 589(Pt 19):4759-4776.

Bodine SC, Latres E, Baumhueter S, Lai VK, Nunez L, Clarke BA, Poueymirou WT, Panaro FJ, Na E, Dharmarajan K, Pan ZQ, Valenzuela DM, DeChiara TM, Stitt TN, Yancopoulos GD, Glass DJ. 2001. Identification of ubiquitin ligases required for skeletal muscle atrophy. Science 294(5547):1704-1708.

Bonaldo P, Sandri M. 2013. Cellular and molecular mechanisms of muscle atrophy. Disease models & mechanisms 6(1):25-39.

Bowyer SL, LaMothe MP, Hollister JR. 1985. Steroid myopathy: incidence and detection in a population with asthma. The Journal of allergy and clinical immunology 76(2 Pt 1):234-242.

Braun TP, Grossberg AJ, Krasnow SM, Levasseur PR, Szumowski M, Zhu XX, Maxson JE, Knoll JG, Barnes AP, Marks DL. 2013. Cancer- and endotoxin-induced cachexia require intact glucocorticoid signaling in skeletal muscle. FASEB journal : official publication of the Federation of American Societies for Experimental Biology 27(9):3572-3582.

Braun TP, Marks DL. 2015. The regulation of muscle mass by endogenous glucocorticoids. Frontiers in physiology 6:12.

Braun TP, Zhu X, Szumowski M, Scott GD, Grossberg AJ, Levasseur PR, Graham K, Khan S, Damaraju S, Colmers WF, Baracos VE, Marks DL. 2011. Central nervous system inflammation induces muscle atrophy via activation of the hypothalamic-pituitary-adrenal axis. The Journal of experimental medicine 208(12):2449-2463.

Britto FA, Begue G, Rossano B, Docquier A, Vernus B, Sar C, Ferry A, Bonnieu A, Ollendorff V, Favier FB. 2014. REDD1 deletion prevents dexamethasone-induced skeletal muscle atrophy. American journal of physiology Endocrinology and metabolism 307(11):E983-993.

Brown EJ, Beal PA, Keith CT, Chen J, Shin TB, Schreiber SL. 1995. Control of p70 s6 kinase by kinase activity of FRAP in vivo. Nature 377(6548):441-446.

Brugarolas J, Lei K, Hurley RL, Manning BD, Reiling JH, Hafen E, Witters LA, Ellisen LW, Kaelin WG, Jr. 2004. Regulation of mTOR function in response to hypoxia by REDD1 and the TSC1/TSC2 tumor suppressor complex. Genes Dev 18(23):2893-2904.

Brunn GJ, Hudson CC, Sekulic A, Williams JM, Hosoi H, Houghton PJ, Lawrence JC, Jr., Abraham RT. 1997. Phosphorylation of the translational repressor PHAS-I by the mammalian target of rapamycin. Science 277(5322):99-101.

Carroll TB, Findling JW. 2010. The diagnosis of Cushing's syndrome. Reviews in endocrine & metabolic disorders 11(2):147-153.

Chromiak JA, Vandenburgh HH. 1992. Glucocorticoid-induced skeletal muscle atrophy in vitro is attenuated by mechanical stimulation. The American journal of physiology 262(6 Pt 1):C1471-1477.

Clarke BA, Drujan D, Willis MS, Murphy LO, Corpina RA, Burova E, Rakhilin SV, Stitt TN, Patterson C, Latres E, Glass DJ. 2007. The E3 Ligase MuRF1 degrades myosin heavy chain protein in dexamethasone-treated skeletal muscle. Cell metabolism 6(5):376-385.

Cohen S, Brault JJ, Gygi SP, Glass DJ, Valenzuela DM, Gartner C, Latres E, Goldberg AL. 2009. During muscle atrophy, thick, but not thin, filament components are degraded by MuRF1-dependent ubiquitylation. The Journal of cell biology 185(6):1083-1095.

Cong H, Sun L, Liu C, Tien P. 2011. Inhibition of atrogin-1/MAFbx expression by adenovirus-delivered small hairpin RNAs attenuates muscle atrophy in fasting mice. Human gene therapy 22(3):313-324.

Dennis MD, Coleman CS, Berg A, Jefferson LS, Kimball SR. 2014. REDD1 enhances protein phosphatase 2A-mediated dephosphorylation of Akt to repress mTORC1 signaling. Science signaling 7(335):ra68.

DeYoung MP, Horak P, Sofer A, Sgroi D, Ellisen LW. 2008. Hypoxia regulates TSC1/2-mTOR signaling and tumor suppression through REDD1-mediated 14-3-3 shuttling. Genes Dev 22(2):239-251.

Dittmar KD, Pratt WB. 1997. Folding of the glucocorticoid receptor by the reconstituted Hsp90-based chaperone machinery. The initial hsp90.p60.hsp70-dependent step is sufficient for creating the steroid binding conformation. The Journal of biological chemistry 272(20):13047-13054.

Du J, Mitch WE, Wang X, Price SR. 2000. Glucocorticoids induce proteasome C3 subunit expression in L6 muscle cells by opposing the suppression of its transcription by NF-kappa B. The Journal of biological chemistry 275(26):19661-19666.

Evenson AR, Fareed MU, Menconi MJ, Mitchell JC, Hasselgren PO. 2005. GSK-3beta inhibitors reduce protein degradation in muscles from septic rats and in dexamethasone-treated myotubes. The international journal of biochemistry & cell biology 37(10):2226-2238.

Fang CH, Li BG, James JH, King JK, Evenson AR, Warden GD, Hasselgren PO. 2005. Protein breakdown in muscle from burned rats is blocked by insulin-like growth factor i and glycogen synthase kinase-3beta inhibitors. Endocrinology 146(7):3141-3149.

Favier FB, Costes F, Defour A, Bonnefoy R, Lefai E, Bauge S, Peinnequin A, Benoit H, Freyssenet D. 2010. Downregulation of Akt/mammalian target of rapamycin pathway in skeletal muscle is associated with increased REDD1 expression in response to chronic hypoxia. American journal of physiology Regulatory,

integrative and comparative physiology 298(6):R1659-1666.

Goldberg AL, Tischler M, DeMartino G, Griffin G. 1980. Hormonal regulation of protein degradation and synthesis in skeletal muscle. Federation proceedings 39(1):31-36.

Gwag T, Park K, Kim E, Son C, Park J, Nikawa T, Choi I. 2013. Inhibition of C2C12 myotube atrophy by a novel HSP70 inducer, celastrol, via activation of Akt1 and ERK1/2 pathways. Archives of biochemistry and biophysics 537(1):21-30.

Hickson RC, Davis JR. 1981. Partial prevention of glucocorticoid-induced muscle atrophy by endurance training. The American journal of physiology 241(3):E226-232.

Hu Z, Wang H, Lee IH, Du J, Mitch WE. 2009. Endogenous glucocorticoids and impaired insulin signaling are both required to stimulate muscle wasting under pathophysiological conditions in mice. The Journal of clinical investigation 119(10):3059-3069.

Ichinoseki-Sekine N, Yoshihara T, Kakigi R, Sugiura T, Powers SK, Naito H. 2014. Heat stress protects against mechanical ventilation-induced diaphragmatic atrophy. Journal of applied physiology 117(5):518-524.

Iwata M, Suzuki S, Hayakawa K, Inoue T, Naruse K. 2009. Uniaxial cyclic stretch increases glucose uptake into C2C12 myotubes through a signaling pathway independent of insulin-like growth factor I. Hormone and metabolic research =

Hormon- und Stoffwechselforschung = Hormones et metabolisme 41(1):16-22.

Kadmiel M, Cidlowski JA. 2013. Glucocorticoid receptor signaling in health and disease. Trends in pharmacological sciences 34(9):518-530.

Kamei Y, Miura S, Suzuki M, Kai Y, Mizukami J, Taniguchi T, Mochida K, Hata T, Matsuda J, Aburatani H, Nishino I, Ezaki O. 2004. Skeletal muscle FOXO1 (FKHR) transgenic mice have less skeletal muscle mass, down-regulated Type I (slow twitch/red muscle) fiber genes, and impaired glycemic control. The Journal of biological chemistry 279(39):41114-41123.

Kelleher AR, Kimball SR, Dennis MD, Schilder RJ, Jefferson LS. 2013. The mTORC1 signaling repressors REDD1/2 are rapidly induced and activation of p70S6K1 by leucine is defective in skeletal muscle of an immobilized rat hindlimb. American journal of physiology Endocrinology and metabolism 304(2):E229-236.

Kukreti H, Amuthavalli K, Harikumar A, Sathiyamoorthy S, Feng PZ, Anantharaj R, Tan SL, Lokireddy S, Bonala S, Sriram S, McFarlane C, Kambadur R, Sharma M. 2013. Muscle-specific microRNA1 (miR1) targets heat shock protein 70 (HSP70) during dexamethasone-mediated atrophy. The Journal of biological chemistry 288(9):6663-6678.

Kuo T, Lew MJ, Mayba O, Harris CA, Speed TP, Wang JC. 2012. Genome-wide analysis of glucocorticoid receptor-binding sites in myotubes identifies gene networks modulating insulin signaling. Proceedings of the National Academy of Sciences

of the United States of America 109(28):11160-11165.

Lagirand-Cantaloube J, Offner N, Csibi A, Leibovitch MP, Batonnet-Pichon S, Tintignac LA, Segura CT, Leibovitch SA. 2008. The initiation factor eIF3-f is a major target for atrogin1/MAFbx function in skeletal muscle atrophy. The EMBO journal 27(8):1266-1276.

Lang CH, Lynch CJ, Vary TC. 2010. BCATm deficiency ameliorates endotoxin-induced decrease in muscle protein synthesis and improves survival in septic mice. American journal of physiology Regulatory, integrative and comparative physiology 299(3):R935-944.

Latres E, Amini AR, Amini AA, Griffiths J, Martin FJ, Wei Y, Lin HC, Yancopoulos GD, Glass DJ. 2005. Insulin-like growth factor-1 (IGF-1) inversely regulates atrophy-induced genes via the phosphatidylinositol 3-kinase/Akt/mammalian target of rapamycin (PI3K/Akt/mTOR) pathway. The Journal of biological chemistry 280(4):2737-2744.

Lehmann JF, Warren CG, Scham SM. 1974. Therapeutic heat and cold. Clinical orthopaedics and related research Mar-Apr(99):207-245.

Lin L, Qian Y, Shi X, Chen Y. 2005. Induction of a cell stress response gene RTP801 by DNA damaging agent methyl methanesulfonate through CCAAT/enhancer binding protein. Biochemistry 44(10):3909-3914.

Lofberg E, Gutierrez A, Wernerman J, Anderstam B, Mitch WE, Price SR, Bergstrom J,

Alvestrand A. 2002. Effects of high doses of glucocorticoids on free amino acids, ribosomes and protein turnover in human muscle. European journal of clinical investigation 32(5):345-353.

Luo G, Sun X, Hungness E, Hasselgren PO. 2001. Heat shock protects L6 myotubes from catabolic effects of dexamethasone and prevents downregulation of NF-kappaB. American journal of physiology Regulatory, integrative and comparative physiology 281(4):R1193-1200.

Ma K, Mallidis C, Bhasin S, Mahabadi V, Artaza J, Gonzalez-Cadavid N, Arias J, Salehian B. 2003. Glucocorticoid-induced skeletal muscle atrophy is associated with upregulation of myostatin gene expression. American journal of physiology Endocrinology and metabolism 285(2):E363-371.

Ma XM, Blenis J. 2009. Molecular mechanisms of mTOR-mediated translational control. Nature reviews Molecular cell biology 10(5):307-318.

Manning BD, Cantley LC. 2007. AKT/PKB signaling: navigating downstream. Cell 129(7):1261-1274.

Manring H, Abreu E, Brotto L, Weisleder N, Brotto M. 2014. Novel excitation-contraction coupling related genes reveal aspects of muscle weakness beyond atrophy-new hopes for treatment of musculoskeletal diseases. Frontiers in physiology 5:37.

McGhee NK, Jefferson LS, Kimball SR. 2009. Elevated corticosterone associated with

food deprivation upregulates expression in rat skeletal muscle of the mTORC1 repressor, REDD1. The Journal of nutrition 139(5):828-834.

Menconi M, Gonnella P, Petkova V, Lecker S, Hasselgren PO. 2008. Dexamethasone and corticosterone induce similar, but not identical, muscle wasting responses in cultured L6 and C2C12 myotubes. Journal of cellular biochemistry 105(2):353-364.

Milan G, Romanello V, Pescatore F, Armani A, Paik JH, Frasson L, Seydel A, Zhao J, Abraham R, Goldberg AL, Blaauw B, DePinho RA, Sandri M. 2015. Regulation of autophagy and the ubiquitin-proteasome system by the FoxO transcriptional network during muscle atrophy. Nature communications 6:6670.

Minetto MA, Lanfranco F, Botter A, Motta G, Mengozzi G, Giordano R, Picu A, Ghigo E, Arvat E. 2011. Do muscle fiber conduction slowing and decreased levels of circulating muscle proteins represent sensitive markers of steroid myopathy? A pilot study in Cushing's disease. European journal of endocrinology / European Federation of Endocrine Societies 164(6):985-993.

Morimoto Y, Kondo Y, Kataoka H, Honda Y, Kozu R, Sakamoto J, Nakano J, Origuchi T, Yoshimura T, Okita M. 2015. Heat treatment inhibits skeletal muscle atrophy of glucocorticoid-induced myopathy in rats. Physiological research / Academia Scientiarum Bohemoslovaca 64(6):897-905.

Naito H, Powers SK, Demirel HA, Sugiura T, Dodd SL, Aoki J. 2000. Heat stress

attenuates skeletal muscle atrophy in hindlimb-unweighted rats. Journal of applied physiology 88(1):359-363.

Polge C, Heng AE, Jarzaguet M, Ventadour S, Claustre A, Combaret L, Bechet D, Matondo M, Uttenweiler-Joseph S, Monsarrat B, Attaix D, Taillandier D. 2011. Muscle actin is polyubiquitinylated in vitro and in vivo and targeted for breakdown by the E3 ligase MuRF1. FASEB journal : official publication of the Federation of American Societies for Experimental Biology 25(11):3790-3802.

Protiva P, Hopkins ME, Baggett S, Yang H, Lipkin M, Holt PR, Kennelly EJ, Bernard WI. 2008. Growth inhibition of colon cancer cells by polyisoprenylated benzophenones is associated with induction of the endoplasmic reticulum response. International journal of cancer Journal international du cancer 123(3):687-694.

Proud CG, Denton RM. 1997. Molecular mechanisms for the control of translation by insulin. The Biochemical journal 328 (Pt 2):329-341.

Ramamoorthy S, Cidlowski JA. 2013. Exploring the molecular mechanisms of glucocorticoid receptor action from sensitivity to resistance. Endocrine development 24:41-56.

Revollo JR, Cidlowski JA. 2009. Mechanisms generating diversity in glucocorticoid receptor signaling. Annals of the New York Academy of Sciences 1179:167-178.

Sacheck JM, Ohtsuka A, McLary SC, Goldberg AL. 2004. IGF-I stimulates muscle

growth by suppressing protein breakdown and expression of atrophy-related ubiquitin ligases, atrogin-1 and MuRF1. American journal of physiology Endocrinology and metabolism 287(4):E591-601.

Sandri M. 2008. Signaling in muscle atrophy and hypertrophy. Physiology 23:160-170.

Sandri M, Sandri C, Gilbert A, Skurk C, Calabria E, Picard A, Walsh K, Schiaffino S, Lecker SH, Goldberg AL. 2004. Foxo transcription factors induce the atrophy-related ubiquitin ligase atrogin-1 and cause skeletal muscle atrophy. Cell 117(3):399-412.

Schakman O, Gilson H, Thissen JP. 2008. Mechanisms of glucocorticoid-induced myopathy. The Journal of endocrinology 197(1):1-10.

Seale JP, Compton MR. 1986. Side-effects of corticosteroid agents. The Medical journal of Australia 144(3):139-142.

Selsby JT, Dodd SL. 2005. Heat treatment reduces oxidative stress and protects muscle mass during immobilization. American journal of physiology Regulatory, integrative and comparative physiology 289(1):R134-139.

Senf SM. 2013. Skeletal muscle heat shock protein 70: diverse functions and therapeutic potential for wasting disorders. Frontiers in physiology 4:330.

Senf SM, Dodd SL, McClung JM, Judge AR. 2008. Hsp70 overexpression inhibits NF-kappaB and Foxo3a transcriptional activities and prevents skeletal muscle atrophy. FASEB journal : official publication of the Federation of American

Societies for Experimental Biology 22(11):3836-3845.

Shah OJ, Kimball SR, Jefferson LS. 2000. Acute attenuation of translation initiation and protein synthesis by glucocorticoids in skeletal muscle. American journal of physiology Endocrinology and metabolism 278(1):E76-82.

Shi H, Scheffler JM, Zeng C, Pleitner JM, Hannon KM, Grant AL, Gerrard DE. 2009. Mitogen-activated protein kinase signaling is necessary for the maintenance of skeletal muscle mass. American journal of physiology Cell physiology 296(5):C1040-1048.

Shimizu N, Yoshikawa N, Ito N, Maruyama T, Suzuki Y, Takeda S, Nakae J, Tagata Y, Nishitani S, Takehana K, Sano M, Fukuda K, Suematsu M, Morimoto C, Tanaka H. 2011. Crosstalk between glucocorticoid receptor and nutritional sensor mTOR in skeletal muscle. Cell metabolism 13(2):170-182.

Shoshani T, Faerman A, Mett I, Zelin E, Tenne T, Gorodin S, Moshel Y, Elbaz S, Budanov A, Chajut A, Kalinski H, Kamer I, Rozen A, Mor O, Keshet E, Leshkowitz D, Einat P, Skaliter R, Feinstein E. 2002. Identification of a novel hypoxia-inducible factor 1-responsive gene, RTP801, involved in apoptosis. Molecular and cellular biology 22(7):2283-2293.

Sofer A, Lei K, Johannessen CM, Ellisen LW. 2005. Regulation of mTOR and cell growth in response to energy stress by REDD1. Molecular and cellular biology 25(14):5834-5845.

Stefanovsky V, Langlois F, Gagnon-Kugler T, Rothblum LI, Moss T. 2006. Growth factor signaling regulates elongation of RNA polymerase I transcription in mammals via UBF phosphorylation and r-chromatin remodeling. Molecular cell 21(5):629-639.

Stitt TN, Drujan D, Clarke BA, Panaro F, Timofeyva Y, Kline WO, Gonzalez M, Yancopoulos GD, Glass DJ. 2004. The IGF-1/PI3K/Akt pathway prevents expression of muscle atrophy-induced ubiquitin ligases by inhibiting FOXO transcription factors. Molecular cell 14(3):395-403.

Tamura Y, Kitaoka Y, Matsunaga Y, Hoshino D, Hatta H. 2015. Daily heat stress treatment rescues denervation-activated mitochondrial clearance and atrophy in skeletal muscle. The Journal of physiology 593(12):2707-2720.

Thompson MG, Thom A, Partridge K, Garden K, Campbell GP, Calder G, Palmer RM. 1999. Stimulation of myofibrillar protein degradation and expression of mRNA encoding the ubiquitin-proteasome system in C(2)C(12) myotubes by dexamethasone: effect of the proteasome inhibitor MG-132. Journal of cellular physiology 181(3):455-461.

Tiao G, Fagan J, Roegner V, Lieberman M, Wang JJ, Fischer JE, Hasselgren PO. 1996. Energy-ubiquitin-dependent muscle proteolysis during sepsis in rats is regulated by glucocorticoids. The Journal of clinical investigation 97(2):339-348.

Tintignac LA, Lagirand J, Batonnet S, Sirri V, Leibovitch MP, Leibovitch SA. 2005. Degradation of MyoD mediated by the SCF (MAFbx) ubiquitin ligase. The Journal of biological chemistry 280(4):2847-2856.

Tomas FM, Munro HN, Young VR. 1979. Effect of glucocorticoid administration on the rate of muscle protein breakdown in vivo in rats, as measured by urinary excretion of N tau-methylhistidine. The Biochemical journal 178(1):139-146.

Tsuchida W, Iwata M, Suzuki S, Bannno Y, Inoue T, Matsuo S, Asai Y. 2012. Inhibitory effect of heat stress on glucocorticoid induced skeletal muscle atrophy in relation to heat shock protein expression. Journal of physical therapy (Japanese) 29(7):795-782.

Verhees KJ, Schols AM, Kelders MC, Op den Kamp CM, van der Velden JL, Langen RC. 2011. Glycogen synthase kinase-3beta is required for the induction of skeletal muscle atrophy. American journal of physiology Cell physiology 301(5):C995-C1007.

Wada S, Kato Y, Okutsu M, Miyaki S, Suzuki K, Yan Z, Schiaffino S, Asahara H, Ushida T, Akimoto T. 2011. Translational suppression of atrophic regulators by microRNA-23a integrates resistance to skeletal muscle atrophy. The Journal of biological chemistry 286(44):38456-38465.

Waddell DS, Baehr LM, van den Brandt J, Johnsen SA, Reichardt HM, Furlow JD, Bodine SC. 2008. The glucocorticoid receptor and FOXO1 synergistically

activate the skeletal muscle atrophy-associated MuRF1 gene. American journal of physiology Endocrinology and metabolism 295(4):E785-797.

Wang H, Kubica N, Ellisen LW, Jefferson LS, Kimball SR. 2006. Dexamethasone represses signaling through the mammalian target of rapamycin in muscle cells by enhancing expression of REDD1. The Journal of biological chemistry 281(51):39128-39134.

Welc SS, Phillips NA, Oca-Cossio J, Wallet SM, Chen DL, Clanton TL. 2012. Hyperthermia increases interleukin-6 in mouse skeletal muscle. American journal of physiology Cell physiology 303(4):C455-466.

Wing SS, Goldberg AL. 1993. Glucocorticoids activate the ATP-ubiquitin-dependent proteolytic system in skeletal muscle during fasting. The American journal of physiology 264(4 Pt 1):E668-676.

Wright CR, Brown EL, Ward AC, Russell AP. 2015. G-CSF treatment can attenuate dexamethasone-induced reduction in C2C12 myotube protein synthesis. Cytokine 73(1):1-7.

Yaffe D, Saxel O. 1977. Serial passaging and differentiation of myogenic cells isolated from dystrophic mouse muscle. Nature 270(5639):725-727.

Yamamoto D, Maki T, Herningtyas EH, Ikeshita N, Shibahara H, Sugiyama Y, Nakanishi S, Iida K, Iguchi G, Takahashi Y, Kaji H, Chihara K, Okimura Y. 2010. Branched-chain amino acids protect against dexamethasone-induced

soleus muscle atrophy in rats. Muscle & nerve 41(6):819-827.

Yoshihara T, Ichinoseki-Sekine N, Kakigi R, Tsuzuki T, Sugiura T, Powers SK, Naito H. 2015. Repeated exposure to heat stress results in a diaphragm phenotype that resists ventilator-induced diaphragm dysfunction. Journal of applied physiology 119(9):1023-1031.

Yoshihara T, Kobayashi H, Kakigi R, Sugiura T, Naito H. 2016. Heat stress-induced phosphorylation of FoxO3a signalling in rat skeletal muscle. Acta Physiol (Oxf). doi: 10.1111/apha.12735.

Figure

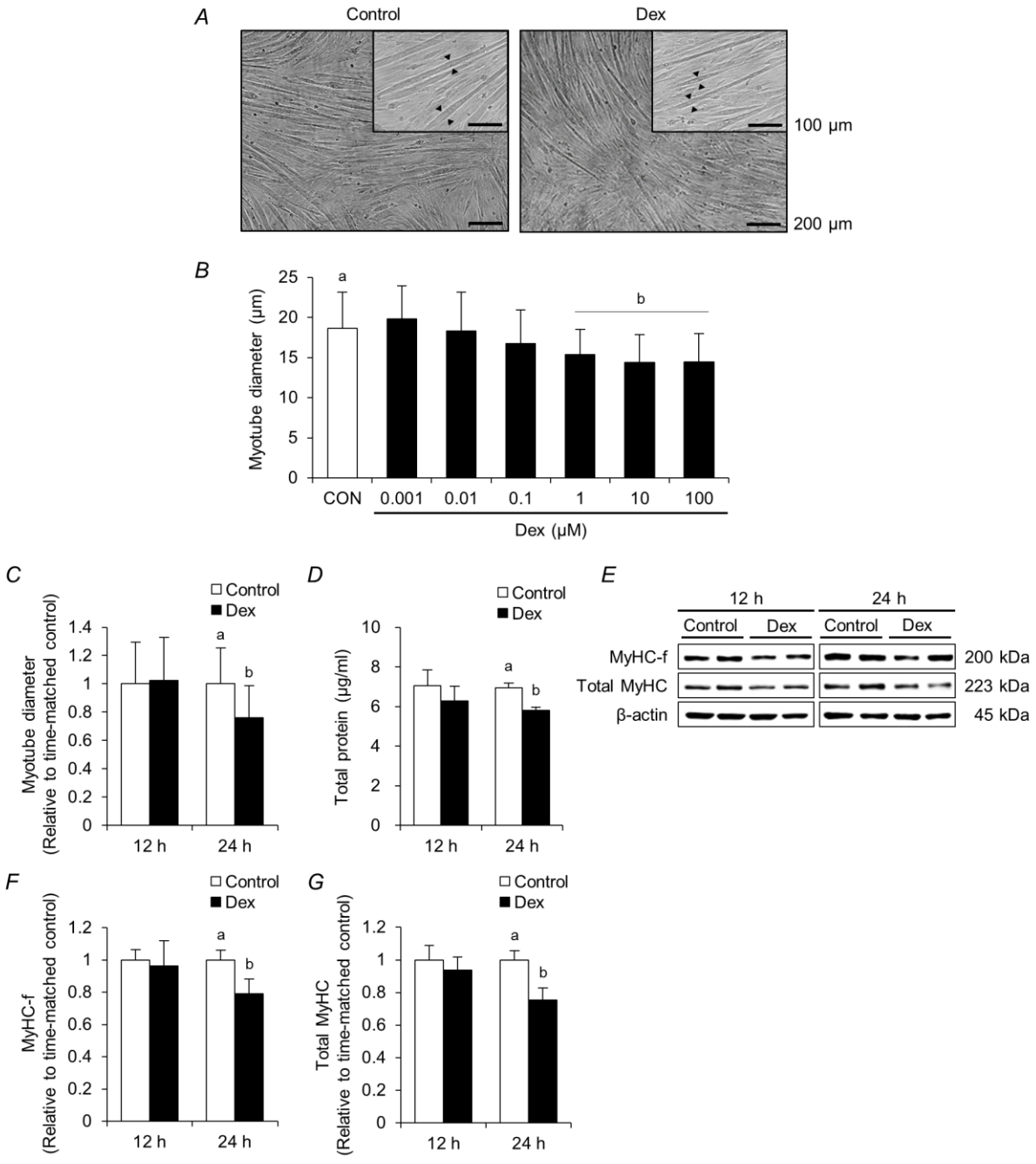

Figure 1. Dex treatment induced atrophic responses in C2C12 myotubes.

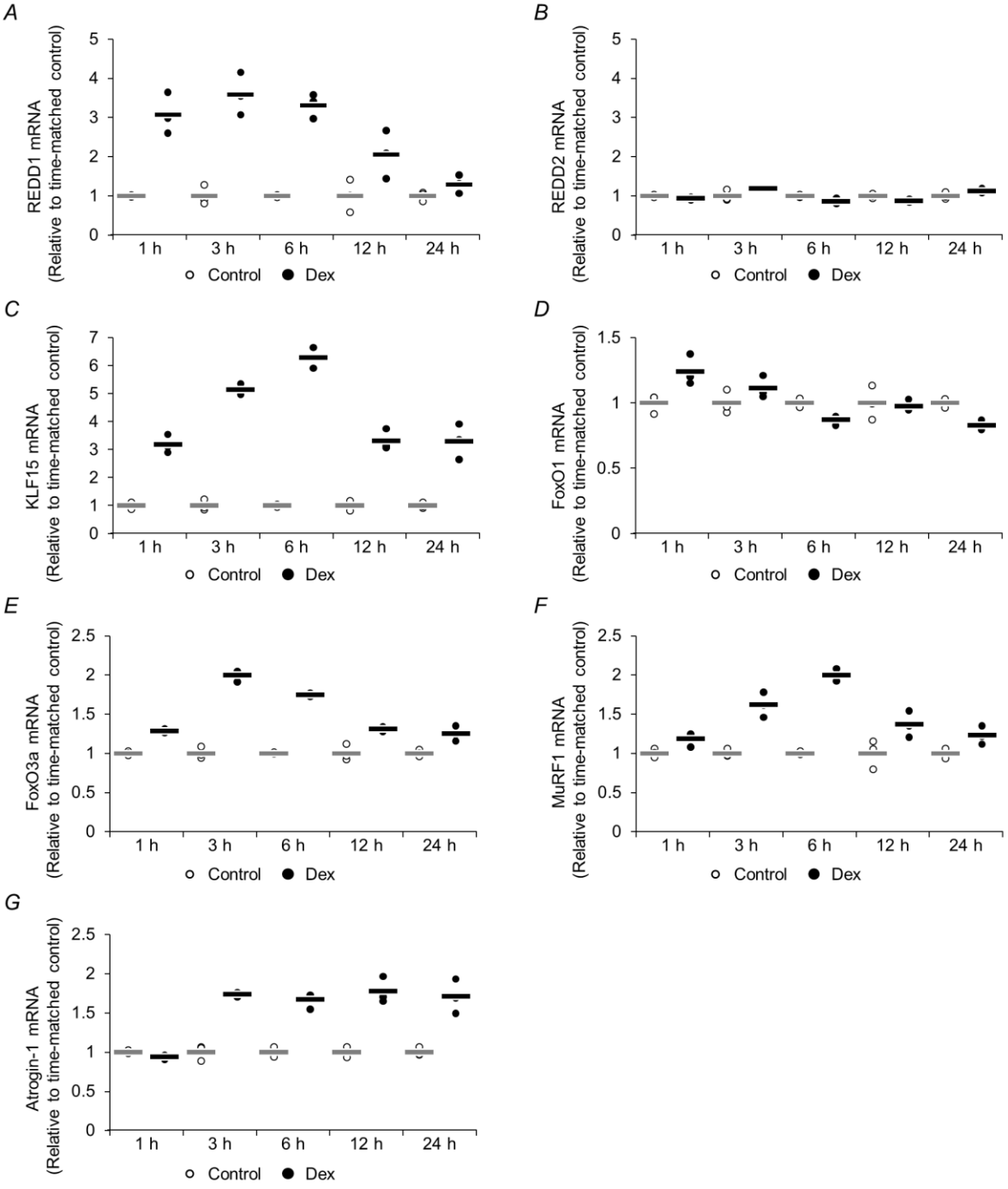

Figure 2. Time course of Dex effects on REDD1, REDD2, KLF15, FoxO1, FoxO3a, MuRF1, and Atrogin-1 mRNA expression in C2C12 myotubes.

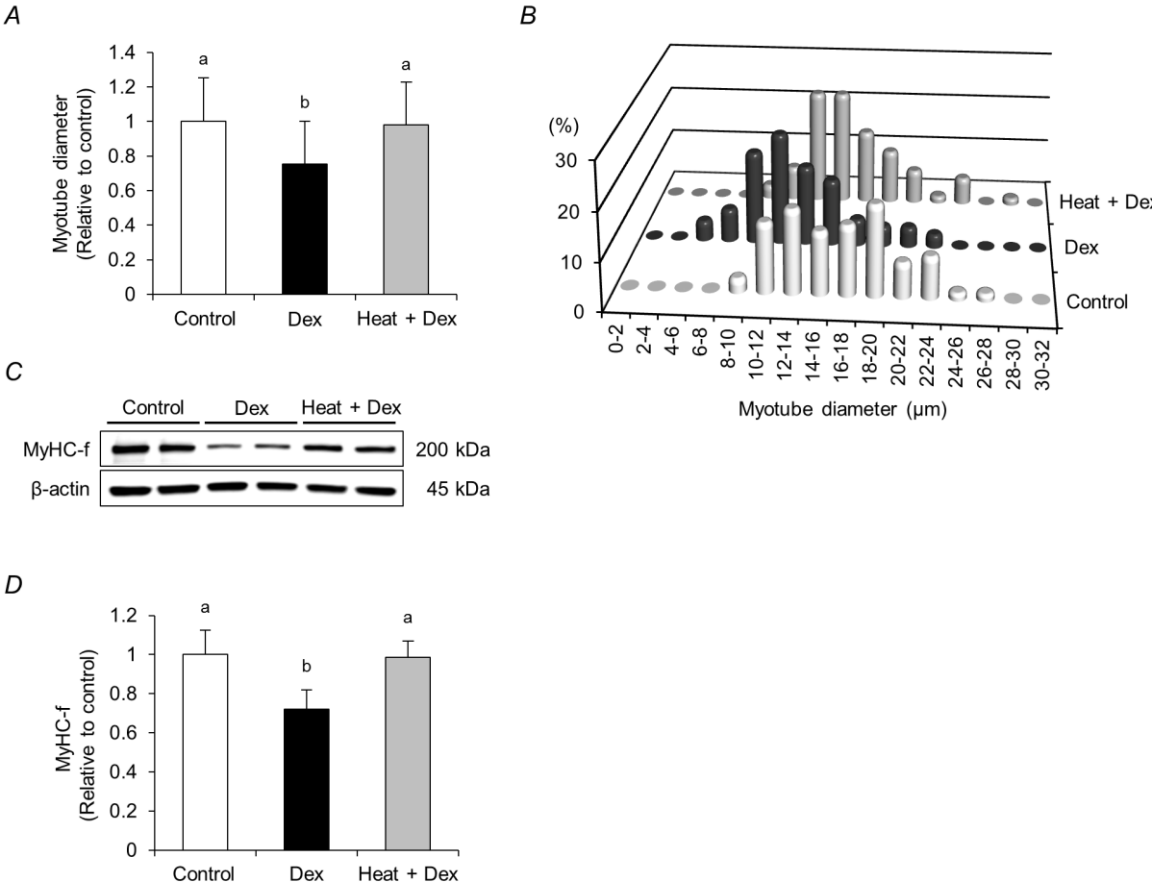

Figure 3. Heat stress suppressed Dex-induced decreases in myotube diameter and MyHC-f content.

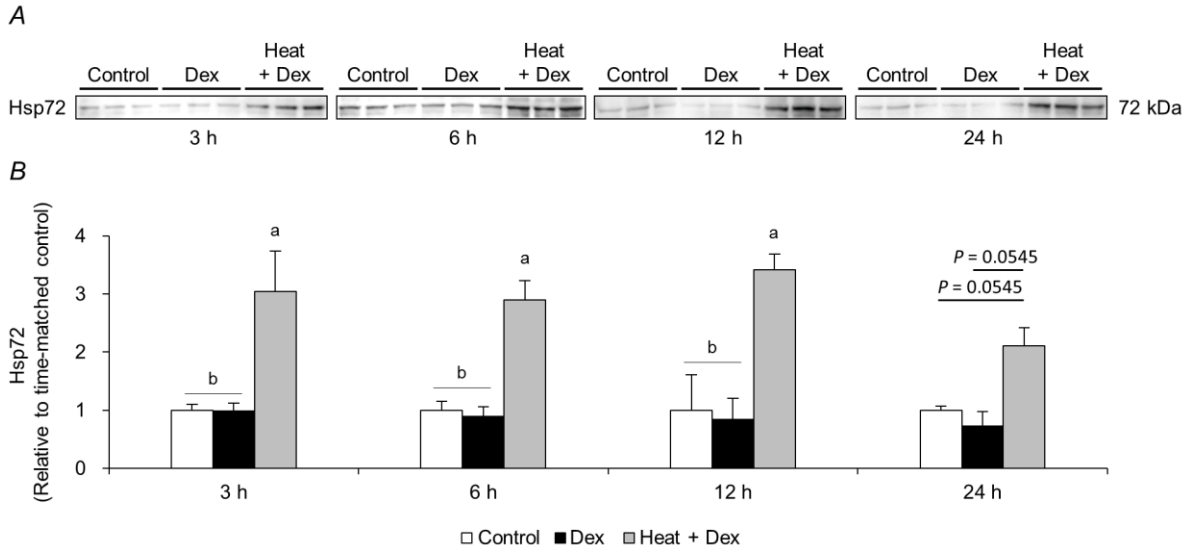

Figure 4. Heat stress increased Hsp72 protein expression in C2C12 myotubes during Dex treatment.

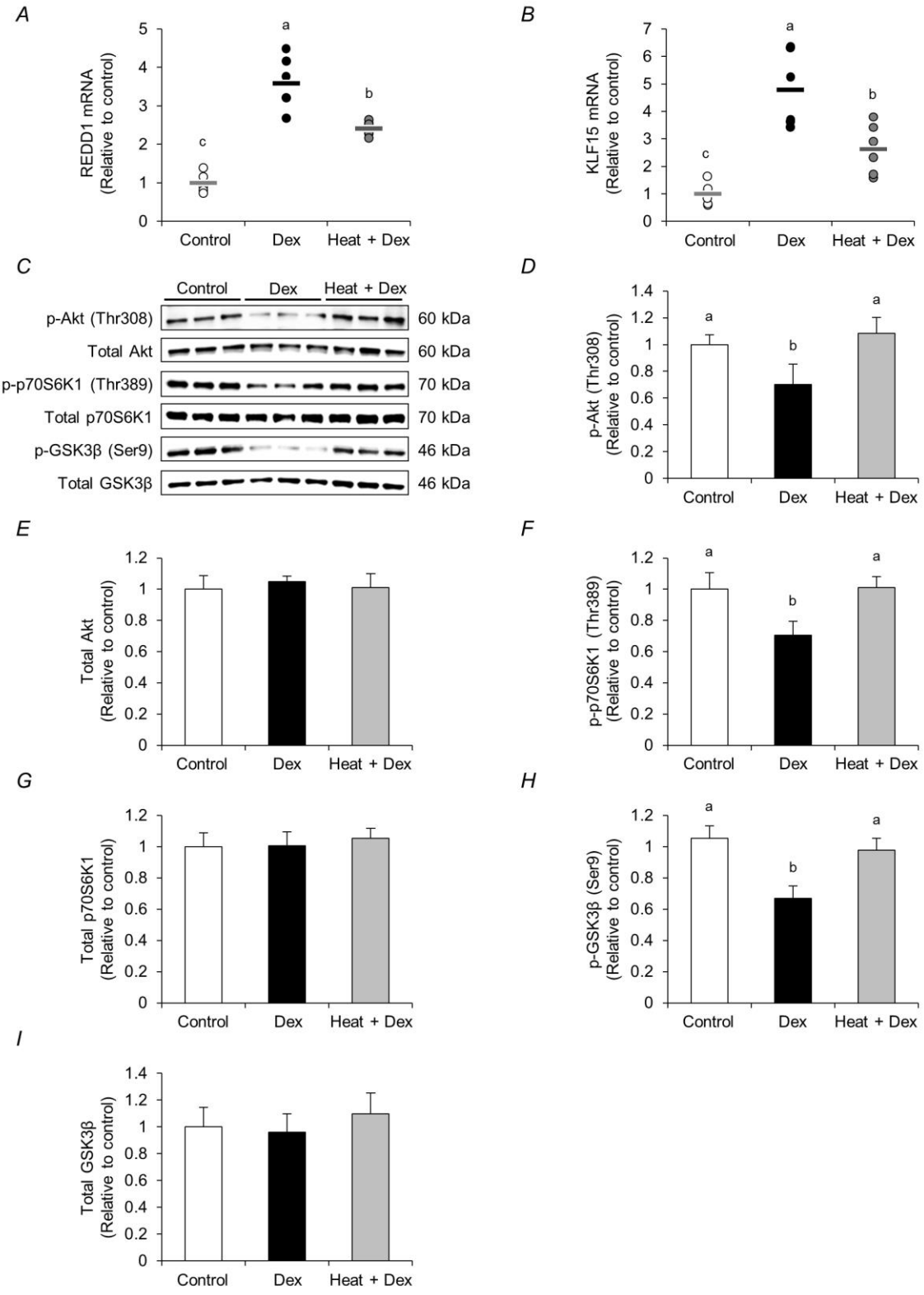

Figure 5. Heat stress normalized Dex-induced increases in REDD1 and KLF15 mRNA expression and decreases in phosphorylated Akt, p70S6K1, and GSK3ß.

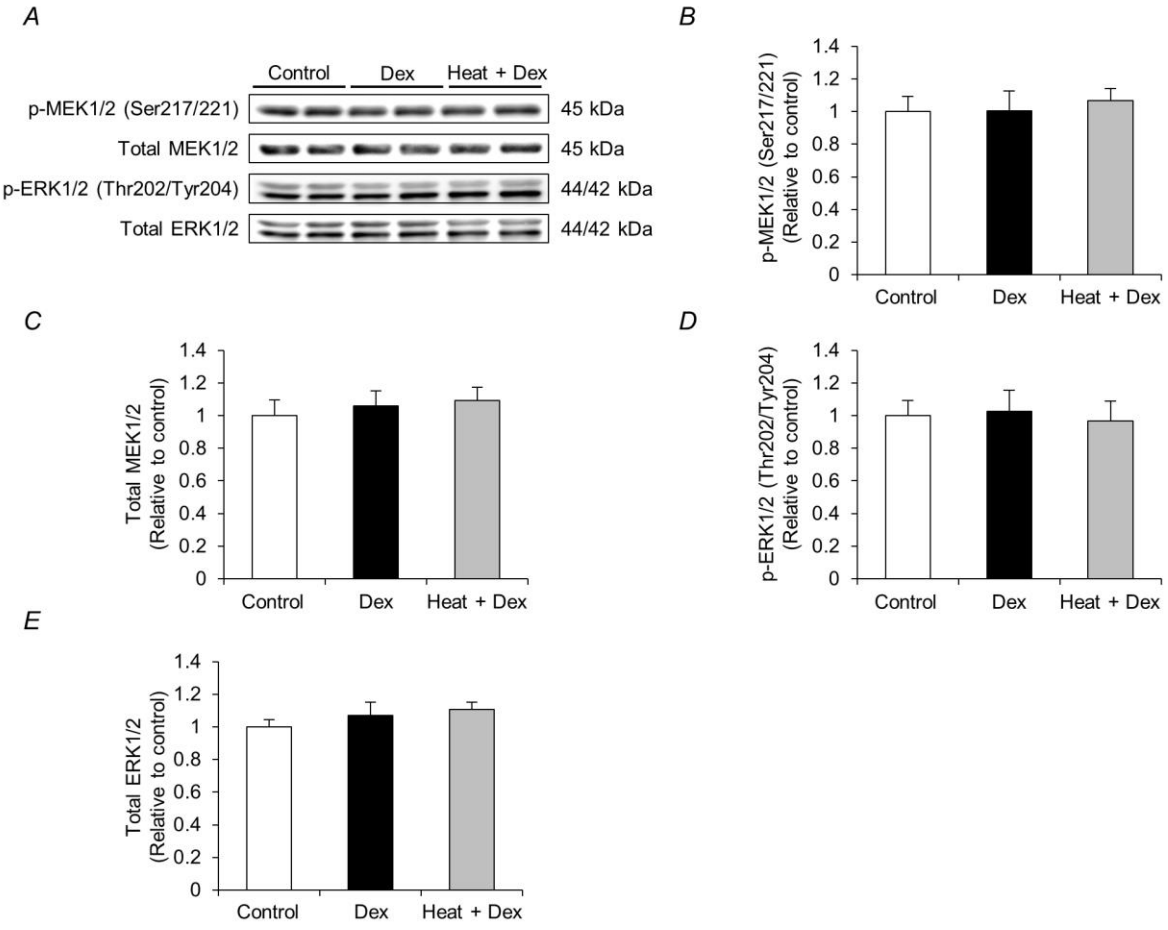

Figure 6. Dex treatment and heat stress did not alter the levels of phosphorylated and total MEK1/2 and ERK1/2.

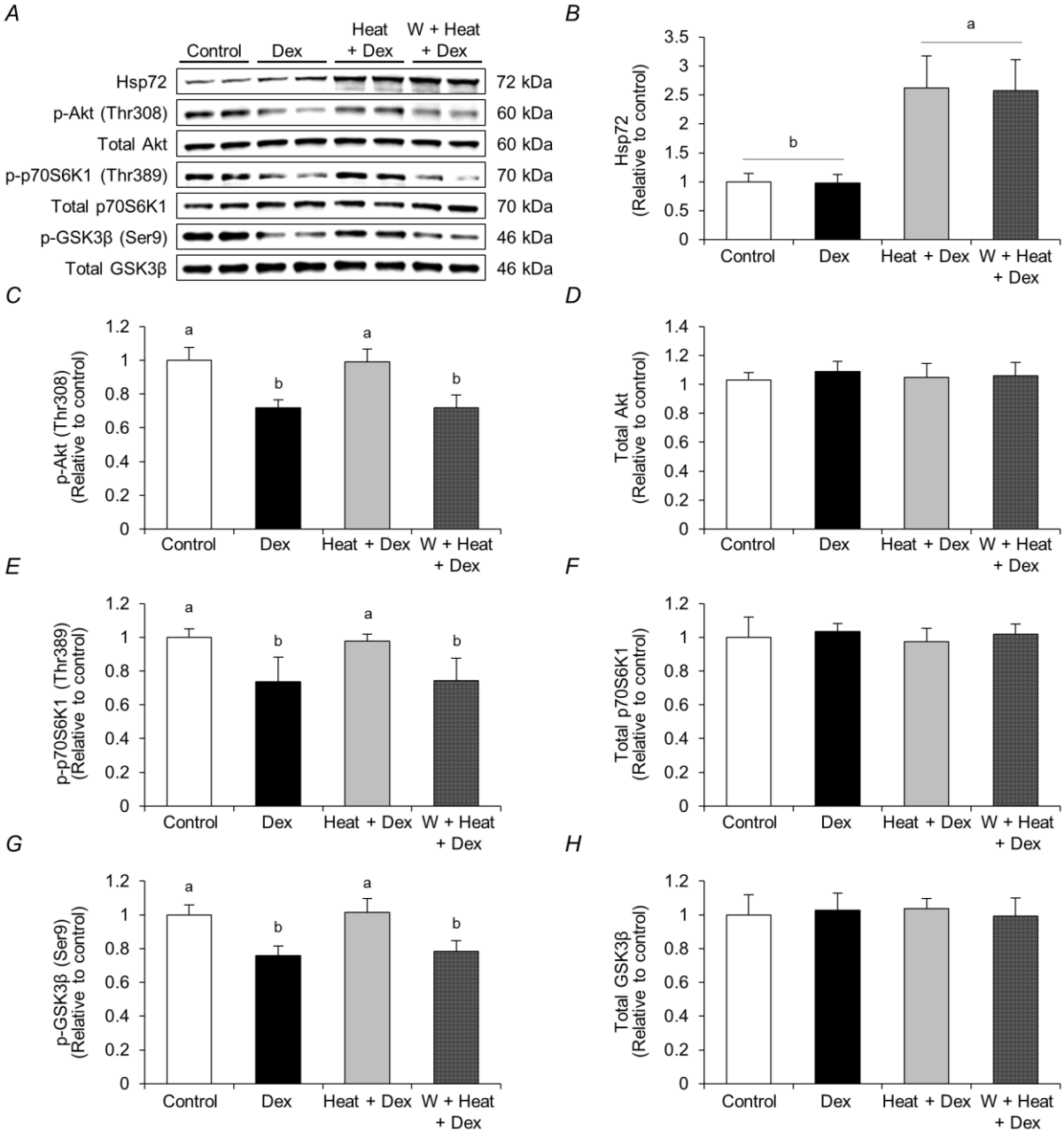

Figure 7. Heat stress normalized Dex-induced decreases in phosphorylated Akt, p70S6K1, and GSK3β through PI3K-dependent mechanisms.

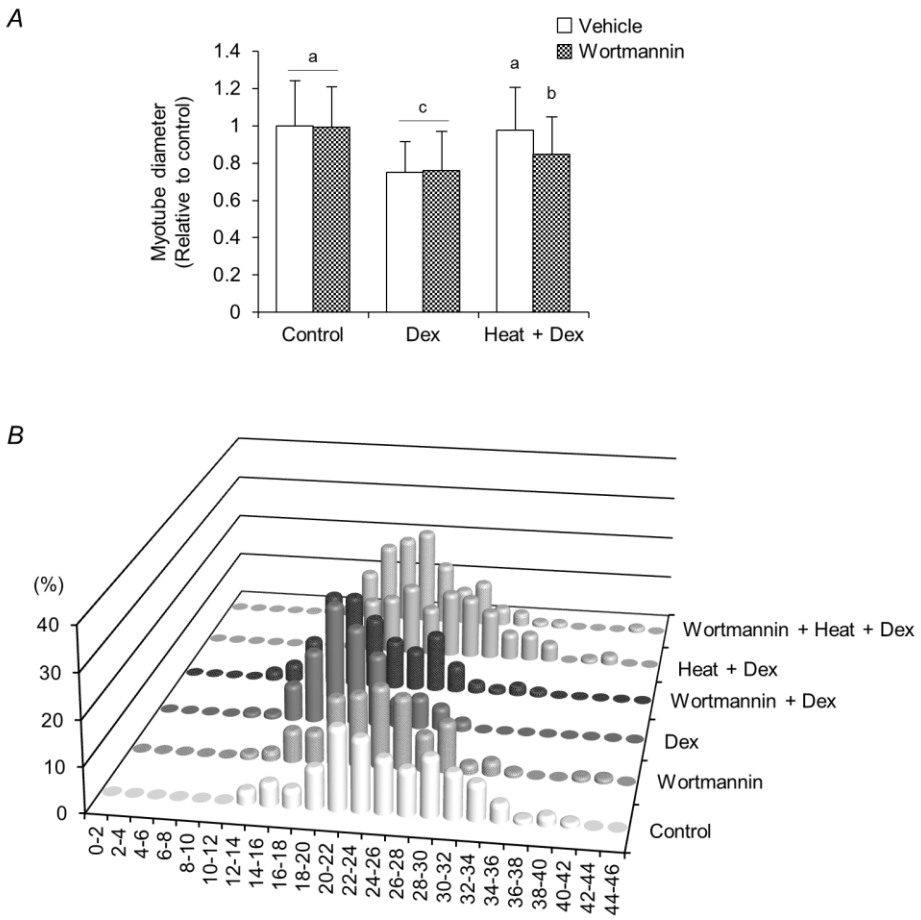

Figure 8. Heat stress attenuated Dex-induced decreases in myotube diameter through PI3K-dependent mechanisms.

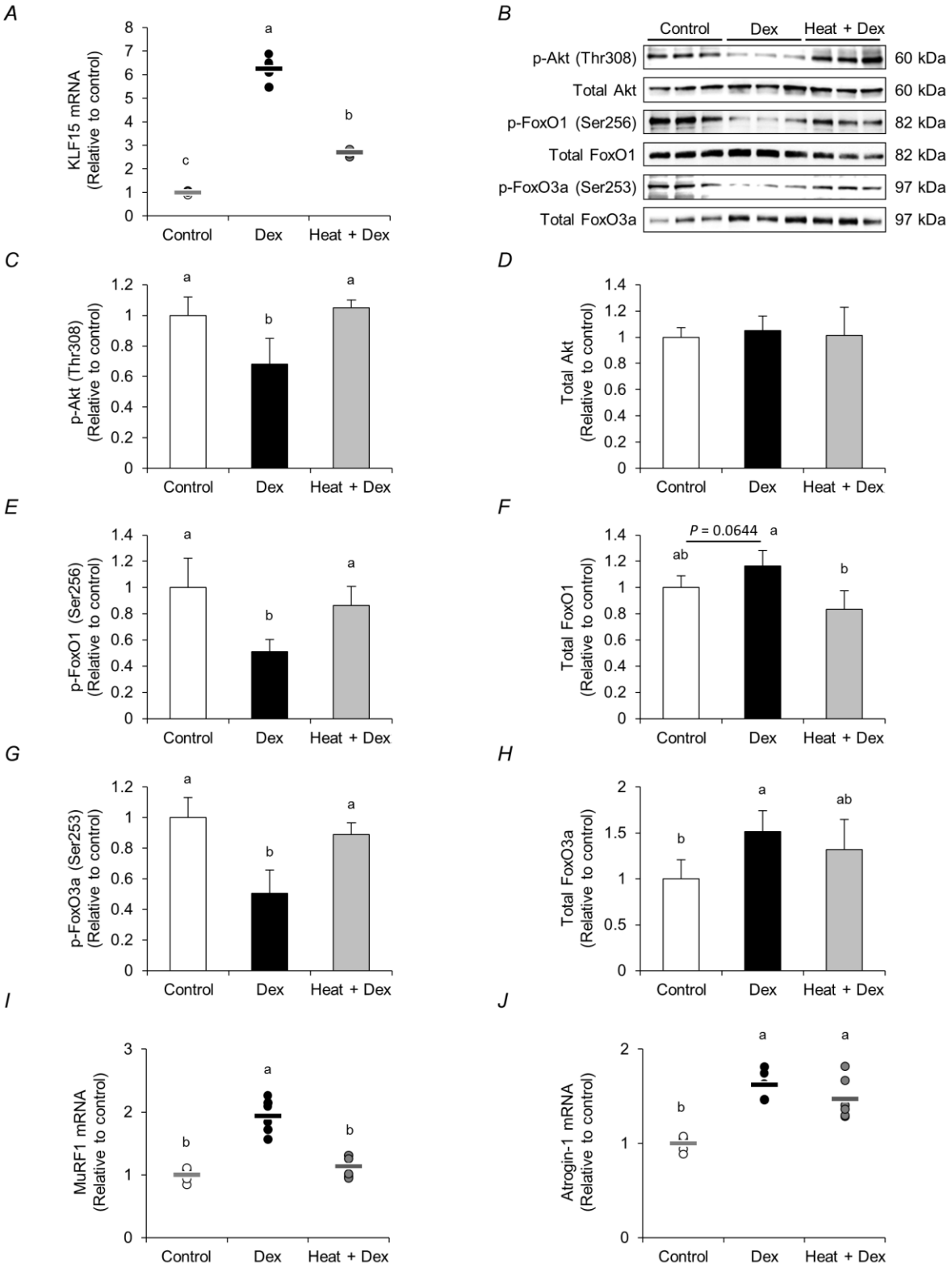

Figure 9. Heat stress normalized Dex-induced increases in REDD1, MuRF1, and Atrogin-1 mRNA expression and decreases in phosphorylated Akt, FoxO1, and FoxO3a.

Figure legends

Figure 1. Dex treatment induced atrophic responses in C2C12 myotubes.

Fully differentiated C2C12 myotubes were treated with the synthetic GC Dex. A, Representative images of C2C12 myotubes were acquired after 24 h treatment with 10 μM Dex. The scale bars represents 100 or 200 μm. B, The graph shows myotube diameters after 24 h Dex treatment at the indicated concentrations. Data are means ± SD ($n \geq 51$ myotubes per condition). C, The graph shows myotube diameters in response to 10 μM Dex treatment for 12 or 24 h. Data are means ± SD ($n \geq 118$ myotubes per condition), relative to the mean value of the control condition, that was set as 1. D, The graph shows total protein content in response to 10 μM Dex ($n = 3$ dishes per condition). Data are means ± SD ($n = 3$ dishes per condition). E-G, Effects of treatment with 10 μM Dex on MyHC-f and total MyHC content were measured by western blot analysis. ß-Actin was used as a protein loading control. MyHC-f and total MyHC content are expressed as means ± SD ($n = 4$ dishes per condition). a and b indicate significant differences among the designated groups ($P < 0.05$), where a > b.

Figure 2. Time course of Dex effects on REDD1, REDD2, KLF15, FoxO1, FoxO3a, MuRF1, and Atrogin-1 mRNA expression in C2C12 myotubes.

A-G, Fully differentiated C2C12 myotubes were treated with Dex (10 μM) for the indicated times. REDD1, REDD2, KLF15, FoxO1, FoxO3a, MuRF1, and Atrogin-1

mRNA expression were measured by real-time quantitative RT-PCR (open circles, control; filled circles, Dex treated). Horizontal bars indicate mean values (n = 3 dishes per condition), relative to the mean value of the control condition that was set as 1.

Figure 3. Heat stress suppressed Dex-induced decreases in myotube diameter and MyHC-f content.

Fully differentiated C2C12 myotubes were exposed to heating (at 41 °C for 60 min) 6 h prior to adding 10 μM Dex and treating for 24 h. Myotube diameters and MyHC-f contents were measured. The experiment was conducted using three conditions in which C2C12 myotubes were not treated (control), C2C12 myotubes were treated with 10 μM Dex (Dex) and C2C12 myotubes were exposed to heating and then treated with 10 μM Dex (Heat + Dex). A, The graph shows average myotube diameters under the three conditions. Data are means ± SD ($n \geq 69$ myotubes per condition), relative to the mean value of the control condition that was set as 1. The symbols a and b significant difference among the designated groups ($P < 0.01$). B, Frequency histogram showing distribution of myotube diameters. C-D, MyHC-f content measured by western blotting with ß-actin as the protein loading control. MyHC-f content is expressed as means ± SD (n = 7 dishes per condition). a and b indicate significant differences among the designated groups ($P < 0.05$), where a > b.

Figure 4. Heat stress increased Hsp72 protein expression in C2C12 myotubes during Dex treatment.

A-B, Fully differentiated C2C12 myotubes were exposed to heating (at 41 °C for 60 min) 6 h prior to 10 μM Dex treatment for 3, 6, 12, and 24 h, as indicated. The experiment was conducted using three conditions, control, Dex, and Heat + Dex conditions, as described for Fig. 3. Hsp72 protein expression was measured by western blotting. Hsp72 expression is expressed as means ± SD (n = 4-6 dishes per condition), relative to the mean value of the control condition that was set as 1. a and b indicate significant differences among the designated groups ($P < 0.05$), where a > b.

Figure 5. Heat stress normalized Dex-induced increases in REDD1 and KLF15 mRNA expression and decreases in phosphorylated Akt, p70S6K1, and GSK3β.

Fully differentiated C2C12 myotubes were exposed to heating (at 41 °C for 60 min) 6 h prior to 10 μM Dex treatment for 3 h. The experiment was conducted using three conditions, control, Dex, and Heat + Dex, as described for Fig. 3. A-B, REDD1 and KLF15 mRNA expression were measured by real-time quantitative RT-PCR. Horizontal bars indicate mean values (n = 6 dishes per condition), relative to the mean value of the control condition that was set as 1. C-I, Levels of phosphorylated and total Akt, p70S6K1, and GSK3β were measured by western blotting. Data are expressed as means ± SD (n = 6 dishes per condition). a, b, and c indicate significant differences

among the designated groups ($P < 0.05$), where a > b > c.

Figure 6. Dex treatment and heat stress did not alter the levels of phosphorylated and total MEK1/2 and ERK1/2.

Fully differentiated C2C12 myotubes were exposed to heating (at 41 °C for 60 min) 6 h prior to 10 μM Dex treatment for 3 h. The experiment was conducted using three conditions, control, Dex, and Heat + Dex, as described for Fig. 3. A-E, Levels of phosphorylated and total MEK1/2 and ERK1/2 were measured by western blotting. Data are expressed as means ± SD (n = 6 dishes per condition).

Figure 7. Heat stress normalized Dex-induced decreases in phosphorylated Akt, p70S6K1, and GSK3β through PI3K-dependent mechanisms.

Fully differentiated C2C12 myotubes were treated with wortmannin (100 nM) at the indicated concentrations 2 h before heat treatment, and were exposed to heating (at 41 °C for 60 min) 6 h prior to 10 μM Dex treatment for 3 h. Wortmannin was maintained throughout the experiment. The experiment was conducted using four conditions, control, Dex, Heat + Dex, and wortmannin + Heat + Dex (W + Heat + Dex). A-H, Hsp72 protein expression and levels of phosphorylated and total Akt, p70S6K1, and GSK3β were measured by western blotting. Data are expressed as means ± SD (n = 8 dishes per condition), relative to the mean value of the control condition that was set

as 1. a and b indicate significant differences among the designated groups ($P < 0.05$), where a > b.

Figure 8. Heat stress attenuated Dex-induced decreases in myotube diameter through PI3K-dependent mechanisms.

Fully differentiated C2C12 myotubes were treated with 100 nM wortmannin 2 h before heat treatment, and were exposed to heating (at 41 °C for 60 min) 6 h prior to adding 10 μM Dex and treating for 24 h. Wortmannin was maintained throughout the experiment. Myotube diameters were measured. The experiment was conducted using six conditions, control, wortmannin, Dex, wortmannin + Dex, Heat + Dex, and wortmannin + Heat + Dex. A, The graph shows average myotube diameters. Data are means ± SD ($n \geq 110$ myotubes per condition) relative to the mean value of the control condition that was set as 1. a, b, and c indicate significant differences among the designated groups ($P < 0.05$), where a > b > c. B, Frequency histogram showing distribution of myotube diameters.

Figure 9. Heat stress normalized Dex-induced increases in REDD1, MuRF1, and Atrogin-1 mRNA expression and decreases in phosphorylated Akt, FoxO1, and FoxO3a.

Fully differentiated C2C12 myotubes were exposed to heating (at 41 °C for 60 min) 6 h prior to 10 μM Dex treatment for 6 h. The experiment was conducted using three

conditions, control, Dex, and Heat + Dex, as described for Fig. 3. A, KLF15 mRNA expression was measured by real-time quantitative RT-PCR. Horizontal bars indicate mean values (n = 6 dishes per condition), relative to the mean value of the control condition that was set as 1. B-H, Levels of phosphorylated and total Akt, FoxO1, and FoxO3a were measured by western blotting. Data are expressed as means ± SD (n = 6 dishes per condition). I-J, MuRF1 and Atrogin-1 mRNA expression were measured by real-time quantitative RT-PCR. Horizontal bars indicate mean values (n = 6 dishes per condition). a, b, and c significant differences among the designated groups ($P < 0.05$), where a > b > c and ab is not different to a or b.

Supplemental Information

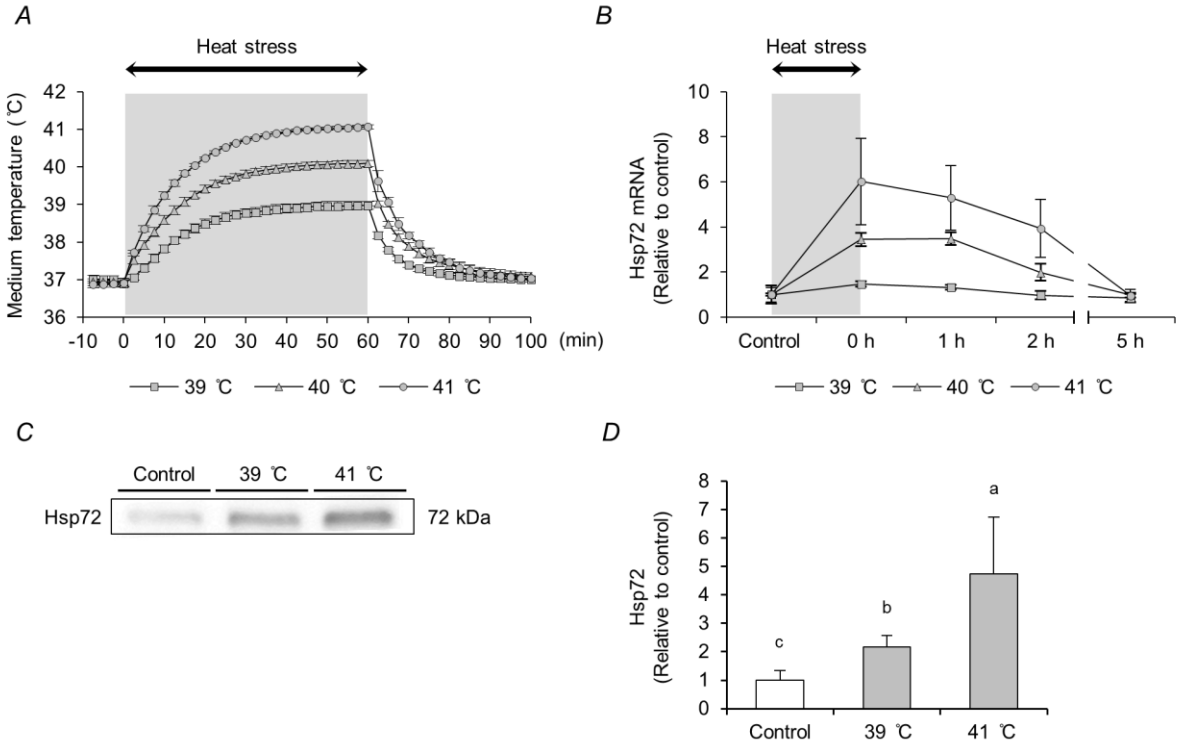

Supplemental Figure S1. Time course of culture medium temperatures and temperature-dependent Hsp72 mRNA and protein expression in C2C12 myotubes.

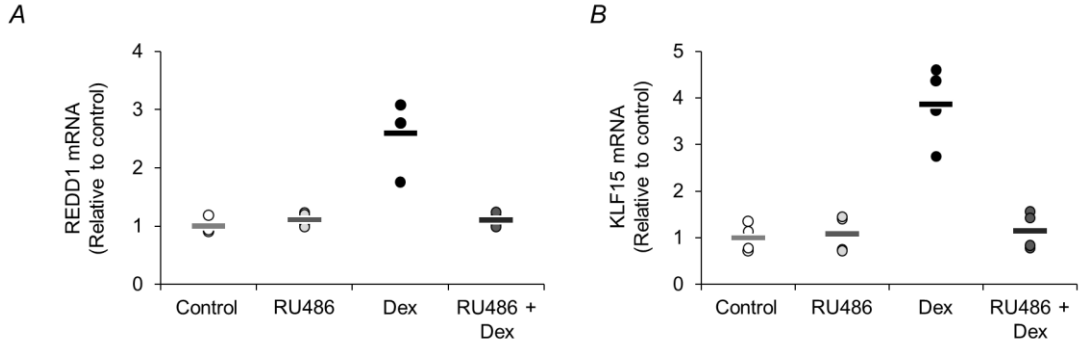

Supplemental Figure S2. GC receptor-dependent REDD1 and KLF15 mRNA expression in C2C12 myotubes treated with Dex.

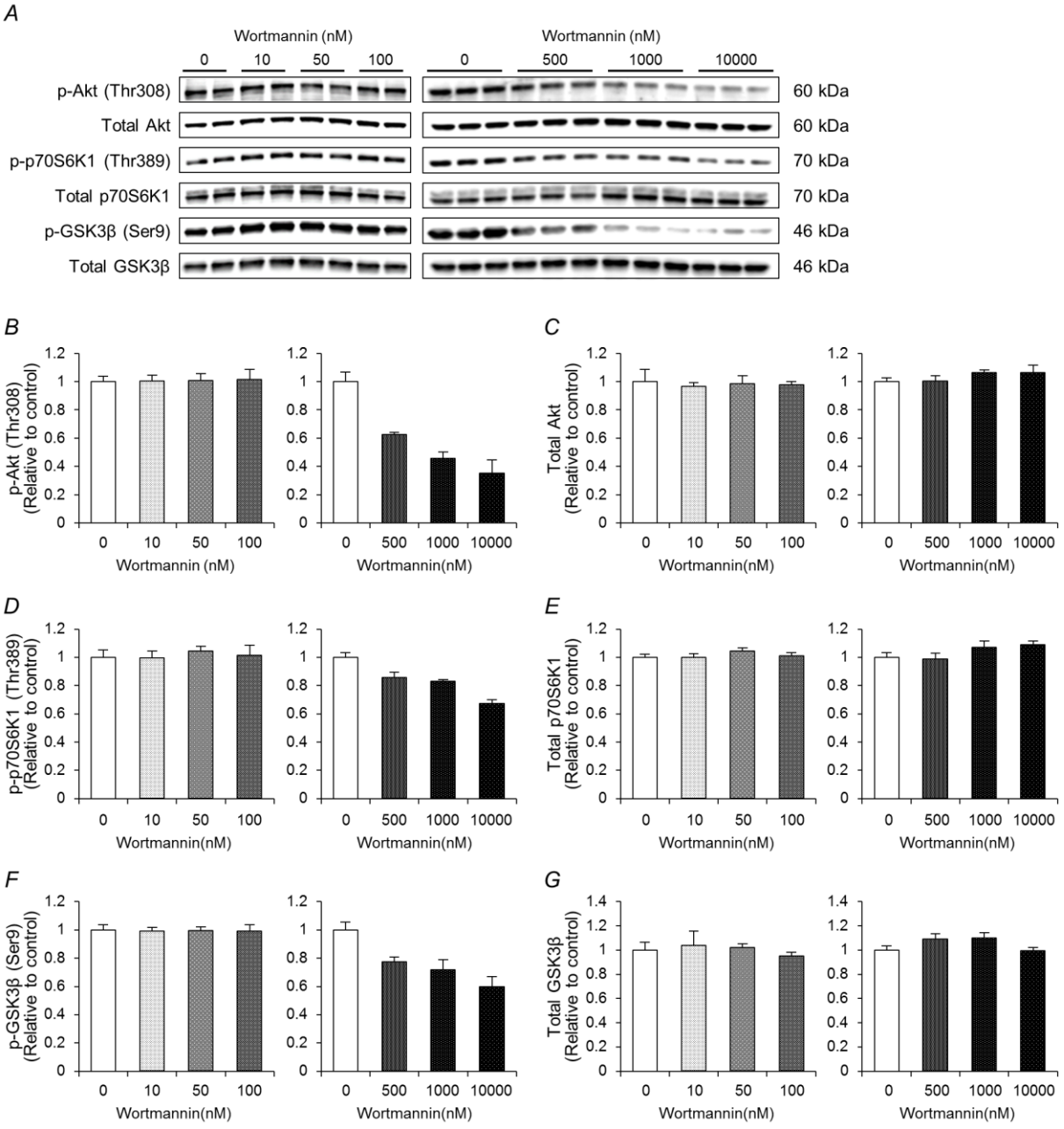

Supplemental Figure S3. Wortmannin treatment inhibited phosphorylated Akt, p70S6K1, and GSK3β in C2C12 myotubes.

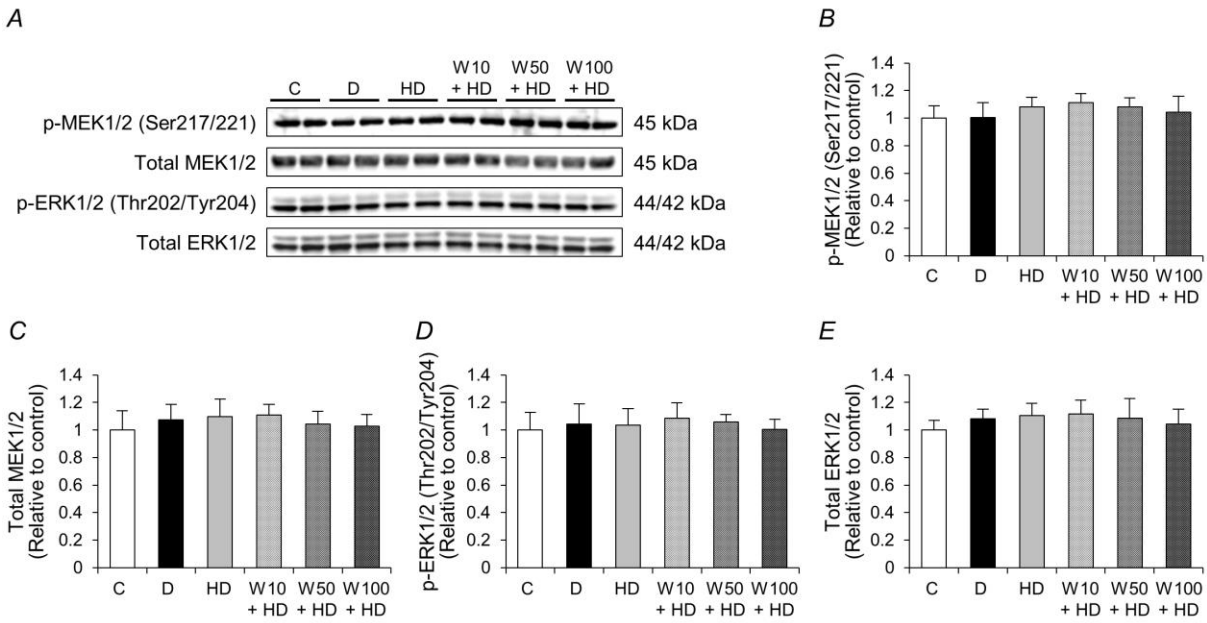

Supplemental Figure S4. Wortmannin treatment did not alter the levels of phosphorylated and total MEK1/2 and ERK1/2 in Dex-treated C2C12 myotubes with/without heat stress.

Supplemental Figure legends

Supplemental Information

Supplemental Figure S1. Time course of culture medium temperatures and temperature-dependent Hsp72 mRNA and protein expression in C2C12 myotubes.

A, 60-mm culture dishes, each containing 4 ml culture medium, were exposed to heat at 39, 40, or 41 °C for 60 min and culture medium temperatures were measured with a thermocouple thermometer with needle type temperature sensor (PTC-301, Unique Medical, Tokyo, Japan) placed in the center of the culture dish. Culture medium temperatures were monitored every 2.5 min from 5 min before heat treatment to 40 min after heat treatment. Data are means ± SD (n = 3 dishes per condition), relative to the mean value of the control condition that was set as 1. B, Fully differentiated C2C12 myotubes were exposed to heating at 39, 40, or 41 °C for 60 min and Hsp72 mRNA expression was measured at the indicated times after heat treatment. Data are means ± SD (n = 4 dishes per condition). C-D, Fully differentiated C2C12 myotubes were exposed to heat at 39 or 41 °C for 60 min. Hsp72 expression was measured at 6 h after heat treatment by western blotting. Hsp72 expression is presented as means ± SD (n = 5 dishes per condition). a, b, and c significant differences among the designated groups ($P < 0.05$), where a > b > c.

Supplemental Figure S2. GC receptor-dependent REDD1 and KLF15 mRNA expression

in C2C12 myotubes treated with Dex.

A-B, Fully differentiated C2C12 myotubes were treated with GC receptor (GR) antagonist RU486 (10 μM) and the synthetic GC Dex (10 μM) for 6 h. REDD1 and KLF15 mRNA were measured by real-time quantitative RT-PCR. Horizontal bars indicate mean values (n = 4 dishes per condition), relative to the mean value of the control condition that was set as 1.

Supplemental Figure S3. Wortmannin treatment inhibited phosphorylated Akt, p70S6K1, and GSK3β in C2C12 myotubes.

A-G, Fully differentiated C2C12 myotubes were treated with wortmannin at the indicated concentrations for 12 h. Levels of phosphorylated and total Akt, p70S6K1, and GSK3β were measured by western blotting. Data are means ± SD (n = 3 dishes per condition), relative to the mean value of the control condition that was set as 1.

Supplemental Figure S4. Wortmannin treatment does not alter the levels of phosphorylated and total MEK1/2 and ERK1/2 in Dex-treated C2C12 myotubes with/without heat stress.

Fully differentiated C2C12 myotubes were treated with wortmannin (100 nM) at the indicated concentrations 2 h before heat treatment, and were exposed to heating (at 41 °C for 60 min) 6 h prior to 10 μM Dex treatment for 3 h. Wortmannin was

maintained throughout the experiment. The experiment was conducted using four conditions, control (C), Dex (D), Heat + Dex (HD), 10 μM wortmannin + Heat + Dex (W10 + HD), 50 μM wortmannin + Heat + Dex (W50 + HD), and 100 μM wortmannin + Heat + Dex (W100 + HD). A-E, Levels of phosphorylated and total MEK1/2 and ERK1/2 were measured by western blotting. Data are expressed as means ± SD (n = 8 dishes per condition), relative to the mean value of the control condition that was set as 1.

Acknowledgements

The authors are grateful to Prof. Shigeyuki Suzuki (Nagoya University, Japan) for providing me this study opportunity, Dr. Masahiro Iwata (Nihon Fukushi University, Japan), Dr. Takayuki Akimoto (Waseda University, Japan), Dr. Shingo Matsuo (Nihon Fukushi University), Dr. Yuji Asai (Nihon Fukushi University) for elaborated guidance and invaluable discussion, Dr. Mitsuharu Okutsu (Nagoya City University, Japan) for his helpful comments, Rina Yuminamochi (Kasugai Municipal Hospital), Tomoe Kumagai (Second Narita Memorial Hospital), Masato Tanaka (Maehara Surgery Orthopedic Surgery), and Yoshita Ohno (Nagoya University) for technical assistance in performing the experiments. This work was supported, in part, by JSPS KAKENHI Grant Numbers 26870691 (WT), 26350639 (MI) from Japan Society for the Promotion of Science (JSPS), and in part by a grant from the Public Advertisement Research Project of Nihon Fukushi University.

Competing interests

The authors declare that they have no competing interests.